

Department of
Civil Engineering

College of Engineering
The University of Iowa
Iowa City, Iowa

**Time-Dependent Deformation
of Non-Composite and
Composite Sand-Lightweight
Prestressed Concrete Structures**

by

D.E. Branson

B.L. Meyers

K.M. Kripanarayanan

Phase 1

Report No. 69-1

Prepared Under Iowa
Highway Commission

Grant No. HR-137

TA1
Io9r
69-1

February, 1969

IOWA HIGHWAY COMMISSION

800 LINCOLN WAY
AMES, IOWA 50010

TIME-DEPENDENT DEFORMATION OF NON-COMPOSITE AND COMPOSITE
SAND-LIGHTWEIGHT PRESTRESSED CONCRETE STRUCTURES

PHASE 1

By

D. E. Branson

B. L. Meyers

K. M. Kripanarayanan

Department of Civil Engineering
University of Iowa
Iowa City

February 1969

IOWA STATE HIGHWAY COMMISSION
LIBRARY

FOREWORD

This is a report of research conducted under Phase 1 of the Iowa State Highway Commission Research Project No. HR-137. The project was initiated in February 1968.

This project is being coordinated with the Iowa State Highway Commission Research Project No. HR-136, "Creep and Shrinkage Properties of Lightweight Concrete Used in the State of Iowa" (see report dated October 1968); and with the Iowa Highway Research Board Project No. HR-104, "Evaluation of Experimental Data Obtained from Lightweight Aggregate Bridge Girders" (see report dated August 1968).

Acknowledgement is made of the assistance of Messrs. S. E. Roberts, Research Engineer, Y. H. Gee, Assistant Bridge Engineer, and J. A. Young, Research Technician, of the Iowa Highway Commission; and Mr. J. H. Boehmler, Jr., President, Prestressed Concrete of Iowa, Inc.

ABSTRACT

Presented in this report is an investigation of the use of "sand-lightweight" concrete in prestressed concrete structures. The sand-lightweight concrete consists of 100% sand substitution for fines, along with Idealite coarse and medium lightweight aggregate and Type I Portland Cement.

The study is divided into three parts: a materials study of the concrete itself, a laboratory study of the behavior of both non-composite (5 beams) and composite (4 beams) prestressed beams, and the field measurement of camber of prestressed bridge girders (5 girders). The test period for the laboratory beams was 5 months, although the data collection is continuing for 3 of the beams. The test period included in this report for the bridge girders was 4 months.

The laboratory beams were designed in three groups (3 beams in each group) to investigate the loss of prestress, initial and time-dependent camber, load-deflection behavior, and effect of different slab casting schedules.

Of principal interest in this Phase I study is the time-dependent behavior of sand-lightweight concrete as a material and as used in prestressed structures. This includes the loss of prestress and camber of members that undergo rather high initial strains (due to both high initial stresses and relatively low modulus of elasticity); the effect of the composite deck in reducing the stress level and corresponding creep rate and loss of prestress; and the effect of the time of casting

the composite slab, since the rate of creep, loss of prestress, and camber growth are quite different before and after the slab is cast.

Design procedures are presented for the following:

1. Calculation of creep and shrinkage of the sand-lightweight concrete of this project at any time after casting, including ultimate values. An indication is also given of the calculation of creep and shrinkage at any time after casting, including ultimate values, for normal weight, sand-lightweight, and all-lightweight concrete in general.

2. Both theoretical and approximate methods for calculating loss of prestress of non-composite and composite prestressed structures.

3. Both theoretical and approximate methods for calculating camber of non-composite and composite prestressed structures.

Results computed by these methods are shown to be in reasonably good agreement with the control specimen data, the laboratory beam data, and the bridge girder data.

Keywords: all-lightweight concrete; beams (structural); bridge girders; camber; composite construction (concrete to concrete); creep (materials); deflection; lightweight concrete; loss of prestress; modulus of elasticity; normal weight concrete; precast concrete; prestressed concrete; sand-lightweight concrete; shrinkage; steel relaxation; strain; stress; structural design; test beams; time-dependent.

TABLE OF CONTENTS

Chapter	Page
List of Tables	vi
List of Figures	vii
Notation	x
INTRODUCTION	1
Statement of the problem	1
Review of literature	1
Objectives and scope	3
DESCRIPTION OF EXPERIMENTAL INVESTIGATION	4
ELASTIC AND STRENGTH PROPERTIES, CREEP AND SHRINKAGE	7
Elastic and strength properties	7
Creep and shrinkage	8
LOSS OF PRESTRESS	17
Prediction of prestress loss	17
Loss of prestress for laboratory beams and bridge girders	22
CAMBER	36
Prediction of camber	36
Measured and computed midspan camber for laboratory beams and bridge girders	41
SAMPLE CALCULATIONS	51
SUMMARY AND CONCLUSIONS	54
REFERENCES	58
APPENDICES	61
Appendix A--Materials and test specimens, Instrumentation and test data	61
Appendix B--Discussion of variables affecting creep and shrinkage	70
Appendix C--Common cases of prestress moment diagrams with formulas for computing camber	80

LIST OF TABLES

Table		Page
1	Concrete properties, temperature and humidity data	5
2	Experimental and computed loss of prestress for laboratory beams and computed loss of prestress for bridge girders	29
3	Computed ultimate loss of prestress at midspan, by terms, for the laboratory beams and bridge girders, using the theoretical Eqs. (20) and (21) with experimental parameters	30
4	Computed ultimate loss of prestress at midspan, by terms, for the laboratory beams and bridge girders, using the approximate Eqs. (22) and (23) with experimental parameters	31
5	Measured and computed midspan camber for laboratory beams and bridge girders	44
6	Computed ultimate midspan camber, by terms, for laboratory beams and bridge girders, using the theoretical Eqs. (24) and (27) with experimental parameters	45
7	Computed ultimate midspan camber, by terms, for laboratory beams and bridge girders, using the approximate Eqs. (29) and (30) with experimental parameters	46
A1	Details of concrete mix and mixing procedure for sand-lightweight concrete used in prestressed beams	62
A2	Details of test beams in groups A, B, and C	63

LIST OF FIGURES

Figure		Page
1	Measured and computed compressive strength versus time curves for the moist cured laboratory beam concrete and steam cured bridge girder concrete	9
2	Creep correction factor for time of initial loading, based on 7 day loading age for moist cured concrete and 2-3 day loading age for steam cured concrete, modified from Jones	9
3	Shrinkage correction factor for minimum member thickness greater than 6", for different drying periods, modified from Jones	9
4	Standard creep and shrinkage curves for sand-lightweight concrete, Eqs. (7) through (10), for 3" or less slump, 40% relative humidity, minimum member thickness of 6" or less	11
5	Creep and shrinkage versus time ratio curves for 20-year normal weight concrete data, from Reference 9	11
6	Measured and computed creep coefficients for the sand-lightweight concrete of groups A, B, and C--slump less than 3", loaded at 7 days, average relative humidity 40%, thickness of specimens 6"	13
7	Measured and computed shrinkage strains for the sand-lightweight concrete of groups A, B, and C--slump less than 3", shrinkage from age 7 days, average relative humidity 40%, thickness of specimens 6"	13
8	Measured and computed steel relaxation for relaxation tests	23
9	Typical measured strain distribution diagrams for the end and midspan sections of Beam B1, and example of experimental prestress loss determined for the end section at 150 days after prestressing	23
10	Measured and computed loss of prestress (by theoretical procedure using Eqs. (20) and (21)) for laboratory beams	25
11	Computed loss of prestress (by theoretical procedure using Eq. (21)) for bridge girders	26

LIST OF FIGURES (Cont'd)

Figure		Page
12	Computed loss of prestress, showing separate effects, for typical compsite laboratory beam and bridge girder (by theoretical procedure--Eq. (21)) versus time. Differential shrinkage is included in shrinkage part	27
13	Measured and computed camber (by theoretical procedure using Eqs. (24) and (27)) for the laboratory beams	42
14	Measured and computed camber (by theoretical procedure using Eq. (27)) for bridge girders	43
A1	Non-composite and composite test beams and location of strain gage points	64
A2	View of laboratory showing beams in foreground and prestressing bed containing additional beams at right	65
A3	Forms for beams in prestressing bed	65
A4	Strain gage indicator and switching and balancing unit used with load cells to measure prestress force	66
A5	Prestressing bed, jacking equipment and beams stored in bed	66
A6	Close-up of jacking equipment, bulkheads, and grips	67
A7	Shrinkage specimens in foreground and 7 beams (1 beam crosswise in foreground). Two additional beams in prestressing bed	67
A8	Two of 4 composite beams. Strain gage points and dial gages can be seen. Strands used in relaxation tests are seen at right	68
A9	Cylinders loaded in creep racks and Whittemore gage used to measure strains of beams and shrinkage and creep specimens	68
B1	Strain components	71
B2	Time-dependent strain variables	73
B3	Creep correction factors for slump, cement content, percent fines, air content, and minimum thickness of member, modified from Jones	75

LIST OF FIGURES (Cont'd)

Figure		Page
B4	Shrinkage correction factors for slump, cement content, percent fines, and air content, modified from Jones	76

NOTATION

1	= subscript denoting cast-in-place slab of composite beam or effect of slab
2	= subscript denoting precast beam
A	= area of section
A_g	= area of gross section, neglecting the steel
A_s	= area of prestress steel
A_t	= transformed area of section
a	= empirical constant determined in the laboratory--see Eq. (2)
a	= distance from end of beam to harped points in 2-point harping case of prestressed concrete beams--see Appendix C. Also see term (7) of Eq. (27)
b	= empirical constant determined in the laboratory--see Eq. (2)
C_s	= creep coefficient defined as ratio of creep strain to initial strain at slab casting
C_t	= creep coefficient at any time t
C_{t1}	= creep coefficient of the composite beam under slab dead load
C_{t2}	= creep coefficient of the precast beam concrete
C_u	= ultimate creep coefficient defined as ratio of ultimate creep strain to initial strain
c	= empirical constant determined in the laboratory--see Eq. (5)
c	= subscript denoting composite section. Also used to designate concrete, such as E_c
D	= differential shrinkage strain in micro inches/inch
d	= empirical constant determined in the laboratory--see Eq. (5)
E	= modulus of elasticity
E_c	= modulus of elasticity of concrete, such as at 28 days or at slab casting, etc

- E_{ci} = modulus of elasticity of concrete at the time of transfer of prestress
 E_s = modulus of elasticity of prestressing steel
 e = empirical constant determined in the laboratory--see Eq. (6)
 e = eccentricity of prestress steel
 e_c = eccentricity of prestress steel at center of beam--see Appendix C. Also used in Eq. (19) etc. to denote eccentricity of prestressed steel in composite section
 e_o = eccentricity of prestress steel at end of beam--see Appendix C
 F = prestress force after losses
 F_o = prestress force at transfer (after elastic losses)
 F_i = initial tensioning force
 ΔF = loss of prestress due to time-dependent effects only (such as shrinkage, creep, steel relaxation). The elastic loss is deducted from the tensioning force to obtain F_o
 ΔF_s = total loss of prestress at slab casting minus the initial elastic loss that occurred at the time of prestressing
 ΔF_u = total ultimate loss of prestress minus the initial elastic loss that occurred at the time of prestressing
 f = empirical constant determined in the laboratory--see Eq. (6)
 f_c = concrete stress at steel c.g.s due to prestress and precast beam dead load
 f_{cd} = concrete stress at steel c.g.s due to differential shrinkage
 f_{cs} = concrete stress at steel c.g.s due to slab dead load (plus diaphragm dead load where applicable)
 f'_c = compressive strength of concrete
 $(f'_c)_t$ = compressive strength of concrete at time t
 $(f'_c)_{28}$ = compressive strength of concrete at 28 days
 $(f'_c)_u$ = ultimate compressive strength of concrete
 f_{si} = initial or tensioning stress in prestressing steel

- f_o = stress in prestressing steel at transfer (after elastic loss)
 f_y = yield strength of steel--defined as 0.1% offset yield strength
 I = moment of inertia (second moment of area)
 I_2 = moment of inertia of precast beam
 I_c = moment of inertia of composite section with transformed slab. The slab is transformed into equivalent precast beam concrete by dividing the slab width by E_{c2}/E_{c1}
 I_g = moment of inertia of gross section, neglecting the steel
 I_t = moment of inertia of transformed section
 i = subscript denoting an initial value
 K = deflection constant. For example, for beams of constant section and uniformly loaded:
 cantilever beam, $K = 1/4$
 simple beam, $K = 5/48$
 hinged-fixed beam (one end continuous), $K = 8/185$
 fixed-fixed beam (both ends continuous), $K = 1/32$
 K_1 = deflection constant for the slab dead load
 K_2 = deflection constant for the precast beam dead load
 L = span length
 M = bending moment. When used as the numerical maximum bending moment, for beams of constant section and uniformly loaded:
 cantilever beam, $(-) M = w L^2/2$
 simple beam, $(+) M = w L^2/8$
 hinged-fixed beam (one end continuous), $(-) M = w L^2/8$
 fixed-fixed beam (both ends continuous), $(-) M = w L^2/12$
 M_1 = maximum bending moment under slab dead load
 M_2 = maximum bending moment under precast beam dead load
 M_{1D} = bending moment between diaphragms--see term (7) of Eq. (27)
 m = modular ratio E_s/E_c at time of slab casting
 n = modular ratio E_s/E_c at release of prestress

- PG_{cp} = prestress gain due to creep under slab dead load at time t
 PG_{ds} = prestress gain due to differential shrinkage at time t
 PG_{el} = elastic prestress gain at slab casting
 PL_{cp1} = prestress loss due to creep prior to slab casting at time t
 PL_{cp2} = prestress loss due to creep after slab casting at time t
 PL_{cp} = prestress loss due to creep at time t
 PL_{el} = prestress loss due to elastic shortening
 PL_r = prestress loss due to steel relaxation at time t
 PL_{sh} = prestress loss due to shrinkage of concrete at time t
 PL_t = total prestress loss at any time t
 PL_u = ultimate prestress loss
 p = steel percentage, A_s/A_g
 Q = differential shrinkage force = $D A_1 E_1$ at time t --see Eq. (19) and Reference 23
 s = subscript refers to slab casting time
 t = time in general, time in hours in Eq. (14), and time in days for all other equations. Also subscript denoting time-dependent such as C_t
 u = subscript denoting ultimate value
 w = unit weight of concrete in pcf
 w = uniformly distributed load
 y_{cs} = distance from centroid of composite section to centroid of cast-in-place slab
 α = ratio of creep coefficient at any time t to ultimate creep coefficient
 α_s = ratio of creep coefficient at slab casting to ultimate creep coefficient
 β = creep correction factor for the precast beam concrete age when loaded--see Fig. 2
 β_s = creep correction factor for the precast beam concrete age when slab cast--see section following Eq. (23)
 Δ = midspan camber (positive) or deflection (negative)

- Δ_u = ultimate midspan camber
 Δ_i = initial midspan camber
 $(\Delta_i)_{1D}$ = initial deflection of the precast beam due to the diaphragm dead load--see term (7) of Eq. (27)
 $(\Delta_i)_1$ = initial deflection under slab dead load
 $(\Delta_i)_2$ = initial deflection under precast beam dead load
 $(\Delta_i)_{DL}$ = dead load deflection
 $(\Delta_i)_{F_0}$ = initial camber due to the initial prestress force F_0
 Δ_t = total camber at any time t
 ϵ_{sh} = shrinkage strain in micro inches/inch at time t
 $(\epsilon_{sh})_u$ = ultimate shrinkage strain in micro inches/inch

INTRODUCTION

Statement of the problem

As a result of the increased use of structural lightweight concrete for precast prestressed bridge girders along with normal weight concrete deck slabs, a need exists for a better understanding of the factors, primarily time-dependent, that affect prestress loss and camber in composite beams of these materials. Of particular interest in this study is the behavior of sand-lightweight (100% sand substitution for fines along with lightweight coarse aggregate) prestressed structures, and the effect of the composite slab on the ultimate loss of prestress and camber.

Review of literature

Shrinkage of concrete is its contraction due to drying and chemical change. Various empirical equations are presented in the literature^{1,2,3} for predicting shrinkage strains. ACI Committee 435⁴ has given a quantitative resume of available information on creep and shrinkage as applied to deflections of reinforced concrete beams.

Concrete undergoes time-dependent deformations under the action of sustained load that are attributed to creep of the concrete. The contributions of Lorman⁵, McHenry⁶, Neville⁷, Ross⁸, and Troxell, et. al.⁹ are noted. Lorman and Ross suggested the use of hyperbolic expressions for predicting creep (used in this report in modified form). McHenry's concept of "superposition technique for creep" is used in this report; for example, in the case of creep under slab dead load. Neville's study of the physical nature of creep is noted. The 20-year data of Troxell,

et. al., (Fig. 4 herein) shows the long time nature of creep and shrinkage of concrete.

A number of creep theories and mechanisms of creep have been reviewed by Neville⁷, Ali and Kessler¹⁰, and Meyers, et. al.¹¹. Meyers and Neville¹² and Pauw and Chai¹³ have summarized the primary factors that influence creep. The influence of size and shape of member on creep and shrinkage was also reported by Hansen and Mattock¹⁴.

The principal articles referred to in this report on the subject of creep and shrinkage of all-lightweight and sand-lightweight concrete are those of Jones, et. al.¹⁵, ACI Committee 213¹⁶, and Pfeifer¹⁷.

Although the behavior of non-composite and composite prestressed beams of normal weight concrete has been studied in References 18 through 24, etc., (most of these referred to non-composite beams only), it appears that no such investigation has been made of composite prestressed members of lightweight concrete.

Sinno²⁵, in his study of lightweight non-composite prestressed bridge girders, concluded that hyperbolic functions can be used to predict loss of prestress and camber (used in modified form in this report). Yang²⁶, in a recent study of lightweight non-composite prestressed beams, concluded that creep under both constant stress and variable stress was proportional to the applied stress within limits up to about 40% of the ultimate strength. Both Branson and Ozell²¹, and Sinno²⁵ have observed that camber tends to reach an ultimate value relatively early compared to creep and shrinkage, because of the offsetting effects of loss of prestress and camber growth due to creep.

Methods used in this study for predicting loss of prestress and camber were based in part on the papers of ACI Committee 435²⁷, and Branson^{21,28}.

Objectives and scope

The principal objective of this investigation is to evaluate experimentally the time-dependent behavior of sand-lightweight prestressed concrete beams, including composite beams, in order to present practical design methods, and an indication of their accuracy, for predicting loss of prestress and camber. The effect of different slab casting schedules is of primary interest.

The creep and shrinkage of sand-lightweight concrete is included in the study along with an indication of the time-dependent behavior of normal weight and all-lightweight concrete.

The study is divided into three parts: a materials study of the sand-lightweight concrete itself, a laboratory study of the behavior of both non-composite (5 beams) and composite (4 beams) prestressed beams, and the field measurement of camber of prestressed bridge girders (5 girders).

The test period for the laboratory beams was 5 months, although the data collection is continuing for 3 of the beams. The test period included in this report for the bridge girders was 4 months.

DESCRIPTION OF EXPERIMENTAL INVESTIGATION

The principal laboratory specimens for Phase 1 of the project consist of three groups of pretensioned beams (3 simply supported 6" by 8" beams, 15' long in each group). Composite slabs were cast on 4 of these 9 prestressed beams. The beams were designed as follows:

Group A--3 non-composite beams with different prestress moments.

Group B--3 beams, two of which are composite beams. The slabs were cast at 4 weeks and 10 weeks after the prestressed beams were cast. The same prestress moment was used for the 3 beams.

Group C--Same as Group B but with a different prestress moment.

The prestressed beams for all three groups of laboratory beams, and also for the bridge girders, are sand-lightweight concrete while the slabs are normal weight concrete. The laboratory beams (moist cured for 3 days) were prestressed at age 7 days, and the bridge girders (steam cured until prestressed) were prestressed at age 2-3 days. The composite bridge deck was cast 9 weeks after the bridge girders were cast.

The concrete properties, temperature, and humidity data are shown in Table 1. The concrete mix and mixing procedure, beam details, and instrumentation are shown in Appendix A (Tables A1 and A2, Fig. A1). The measured steel tensioning stress for the laboratory beams was 172 ± 4 ksi, and the design tensioning stress for the bridge girders was 190 ksi. The ultimate strength and yield strength (0.1% offset) were: for the laboratory beam steel 250 ksi and 235 ksi, respectively, and for the bridge girder steel 270 ksi and 250 ksi, respectively.

1-7 TABLE 1--CONCRETE PROPERTIES, TEMPERATURE AND HUMIDITY DATA

Property	Concrete Batch								
	Gp. A	Gp. B	Gp. C	Slab	Slab	Slab	Slab	6 ^{Bridge}	Bridge
	Lt.Wt	Lt.Wt	Lt.Wt	B2	C2	B3	C3	Lt.Wt	7 ^{Slab}
				N.Wt	N.Wt	N.Wt	N.Wt		N.Wt
f'_c (7 days) psi	6700	5500	6150	--	--	--	--	5600	
f'_c (28 days) psi	9350	8150	8750	4800	4140	5100	4300	6100	3500
Unit Wt (Wet) pcf	124.0	124.0	125.0	--	--	--	--	--	--
U. Wt (Dry-7d)pcf	123.0	123.5	123.5	153	152	152	153	122.0	145
Meas. Air Ent. %	4.0	6.0	6.0	--	--	--	--	--	--
Slump in	2.0	2.5	2.5	2.5	2.5	3.0	2.5	--	--
³ Modulus of Elasticity psi at 7 Days x 10 ⁶	--	--	a. 3.20	--	--	--	--	a. 3.04	--
	--	--	b. 3.33	--	--	--	--	b. 3.10	--
	<u>3.68</u>	<u>3.35</u>	c. <u>3.55</u>	--	--	--	--	c. <u>3.32</u>	--
³ Modulus of Elasticity psi at 28 Days x 10 ⁶	--	--	a. 3.28	--	--	--	--	--	--
	--	--	b. 3.58	--	--	--	--	--	--
	<u>4.35</u>	<u>4.09</u>	c. <u>4.23</u>	<u>4.33</u>	<u>3.97</u>	<u>4.41</u>	<u>4.05</u>	<u>3.47</u>	<u>3.41</u>

1 Lab. temp: 61-85 deg. F., avg. temp. 78 deg. F. Lab. relative humidity: 25-61%, avg. rel. hum. 40%. Avg. rel. hum. for central Iowa (from U.S. Weather Bur.): Jan.-79%, July-66%, Mean Annual 71%. For Spr-Sum-Fall, use 70%.

2 Stress levels for creep tests were approx. design stresses for lab. beams:

Mix	Strength, f'_c , at 7 days	Stress Level for Creep Tests	% of 7d- f'_c
Gp. A	6700 psi	2010 psi	30%
Gp. B	5500	1375	25
Gp. C	6150	1845	30

3 The modulus of elasticity values are as follows: a. Measured secant (to 0.5 f'_c) mod. of el., b. Measured initial tangent mod. of el., c. All values underlined are computed using $E_c = 33 \sqrt{w^3 f'_c}$, psi.

4 Computed values of modulus of elasticity at release for bridge girders:

Girder No.	Age at Release	Strength at Rel.	³ Mod. of El. at Rel.
152	2 days	5160 psi	<u>3.19</u> $\times 10^6$ psi
153	2	4670	<u>3.04</u>
154	2	4685	<u>3.05</u>
155	3	5130	<u>3.19</u>
156	3	4440	<u>2.96</u>

5 Computed mod. of el. of pres. units at time of slab casting, $E_c \times 10^6$ psi: Gp. B --4.10, 4.35; Gp. C--4.25, 4.49; Girders 152, 153, 154--3.50; Girders 155, 156--3.38.

6 Concrete specimens for data in this column obtained from casting yard for Bridge Girders 155 and 156. Measurements made in laboratory.

7 "Design" values were used for bridge slab concrete.

The experimental data for the laboratory specimens consists of the following:

1. Strength properties, elastic properties, shrinkage and creep data, from control specimens.
2. Temperature and humidity data.
3. Initial and time-dependent concrete beam strains. These are used in determining experimental loss of prestress.
4. Steel relaxation data.
5. Initial and time-dependent camber.

Camber data for the bridge girders²⁹ is also included in this report.

Various stages in the preparation and testing of the laboratory specimens are shown in Figs. A2 through A9.

ELASTIC AND STRENGTH PROPERTIES, CREEP AND SHRINKAGE

Elastic and strength properties

The secant, initial tangent, and computed moduli of elasticity (using the well-known Eq. (1)³⁰) for the moist cured laboratory beam concrete and steam cured bridge girder concrete are shown in Table 1.

$$E_c = 33 w^{1.5} \sqrt{f'_c}, \text{ psi; } w \text{ in pcf and } f'_c \text{ in psi} \quad (1)$$

The computed values for the limited number of tests made were from 6% to 15% higher than the initial tangent values. However, the computed modulus of elasticity was used in computing initial camber of the laboratory beams and bridge girders, and these values were in agreement with the measured initial camber data (Table 5). Eq. (1) is considered satisfactory for computing the modulus of elasticity of normal weight, sand-lightweight, and all-lightweight concrete.

A study of concrete compressive strength versus time in this project and References 4, 16, 31, 32 indicates an appropriate general equation in the form of Eq. (2) for predicting compressive strength at any time.

$$(f'_c)_t = \frac{t}{a + bt} (f'_c)_{28d} \quad (2)$$

where a and b are constants, $(f'_c)_{28d}$ = 28-day strength, and t = time.

The following equations are recommended for the sand-lightweight concrete of this project:

Moist cured

$$(f'_c)_t = \frac{t}{5.0 + 0.8t} (f'_c)_{28d}; \text{ or } (f'_c)_u = 1.25 (f'_c)_{28d} \quad (3)$$

Steam cured

$$(f'_c)_t = \frac{t}{0.70 + 0.97t} (f'_c)_{28d}; \text{ or } (f'_c)_u = 1.03 (f'_c)_{28d} \quad (4)$$

where t is age of concrete in days. The results of Eqs. (3) and (4) agree with the experimental results of this project, as shown in Fig. 1.

Creep and shrinkage

The principal variables that affect creep and shrinkage are outlined and discussed in Appendix B12, 13, 15, 17. The correction factors (to be applied to "standard" creep and shrinkage values) proposed by Jones, et. al.¹⁵ for predicting creep and shrinkage of lightweight concrete are modified for the specimens and conditions of this project. These correction factors are presented (except for humidity which is specified separately) in Figs. 2 and 3, and in Appendix B, Figs. B3 and B4 for:

- | | |
|--|---|
| 1.1 Minimum thickness of member | 1.4 Environmental humidity |
| 1.2 Water-cement ratio in the form of slump and cement content | 1.5 Time of initial loading and time initial shrinkage considered |
| 1.3 Mix proportions in the form of percent fines and air content | |

Based largely on information from References 4, 9, 12, 15, 17, 32, 33, and this project, the following general procedure is suggested for predicting creep and shrinkage of normal weight, sand-lightweight, and all-lightweight concrete:

Standard equations

$$C_t = \frac{t^c}{d + t^c} C_u \quad (5)$$

$$\epsilon_{sh} = \frac{t^e}{f + t^e} (\epsilon_{sh})_u \quad (6)$$

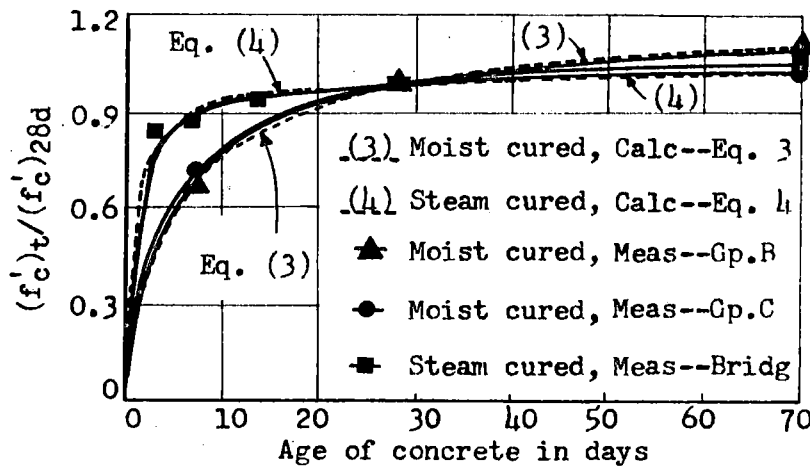


Fig. 1--Measured and computed compressive strength versus time curves for the moist cured laboratory beam concrete and steam cured bridge girder concrete

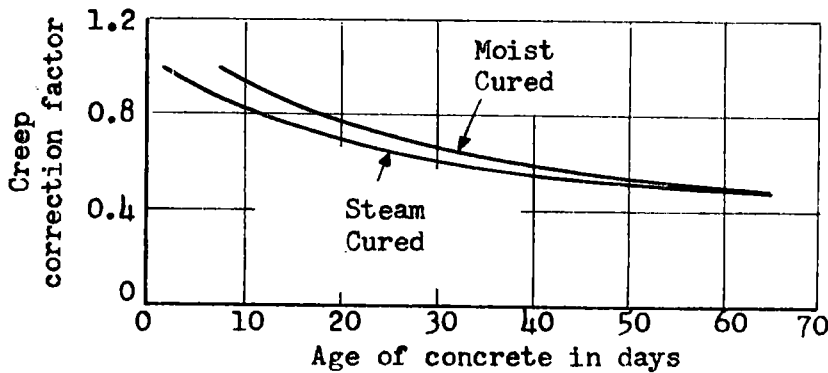


Fig. 2--Creep correction factor for time of initial loading, based on 7 day loading age for moist cured concrete and 2-3 day loading age for steam cured concrete, modified from Jones¹⁵

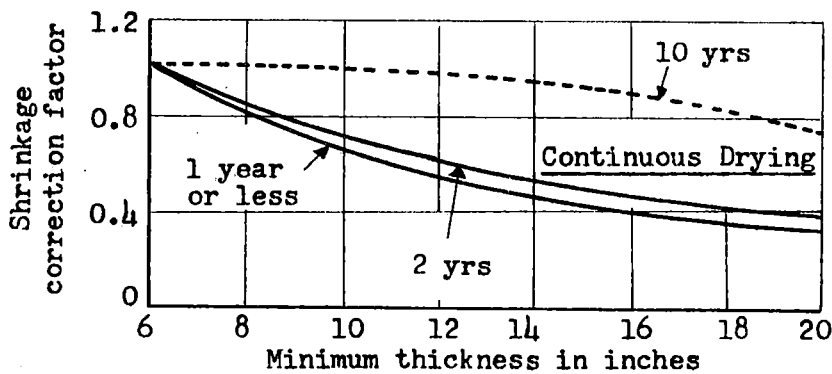


Fig. 3--Shrinkage correction factor for minimum member thickness greater than 6", for different drying periods, modified from Jones¹⁵

where c , d , e , and f are constants, C_u = ultimate creep coefficient, $(\epsilon_{sh})_u$ = ultimate shrinkage strain, and t = time. When the power of t is unity, Eqs. (5) and (6) reduce to the familiar equations of Ross⁸ and Lorman⁵. Primarily because shrinkage takes place more rapidly than creep at early ages (see Fig. 4 in which the normalized shrinkage curves increase more rapidly up to say 200 days than the creep curves), appropriate powers of t are unity for shrinkage and between 1/2 and unity for creep. The distinction becomes relatively important in computing loss of prestress and camber of composite prestressed beams, for example, where the time-dependent behavior before and after the slab is cast is quite different.

Normal ranges of the constants in Eqs. (5) and (6), based on the standard conditions below for both moist cured and steam cured concrete, are^{4, 9, 12, 15, 17, 32}: $c = 1/2$ to 1, $d = 6$ to 30, $C_u = 1.5$ to 3.0, $e = 1$, $f = 20$ to 80, $(\epsilon_{sh})_u = 250$ to 700×10^{-6} in/in.

Based on the results of this study and References 9, 12, 13, 15, 17, 32 and 33 (report of Iowa Highway Project HR-136 dated October 1968), the following design procedures are recommended for predicting creep and shrinkage of the sand-lightweight concrete of this project:

Standard conditions--3" or less slump, 40% ambient relative humidity, minimum thickness of 6" or less

Standard equations--moist cured, 7 day loading age, shrinkage from 7 days

$$C_t = \frac{t^{0.60}}{11.0 + t^{0.60}} C_u, \quad C_u = 1.75 \quad (7)$$

$$\epsilon_{sh} = \frac{t}{23.6 + t} (\epsilon_{sh})_u, \quad (\epsilon_{sh})_u = 590 \times 10^{-6} \text{ in/in} \quad (8)$$

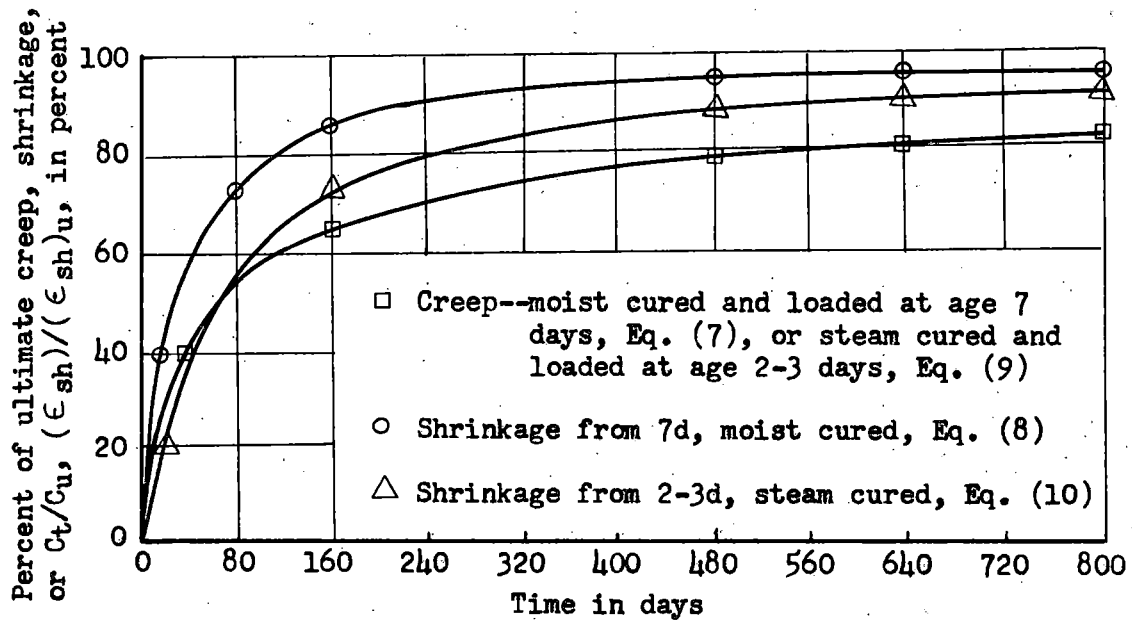


Fig. 4--Standard creep and shrinkage curves for sand-lightweight concrete, Eqs. (7) through (10), for 3" or less slump, 40% relative humidity, minimum member thickness of 6" or less

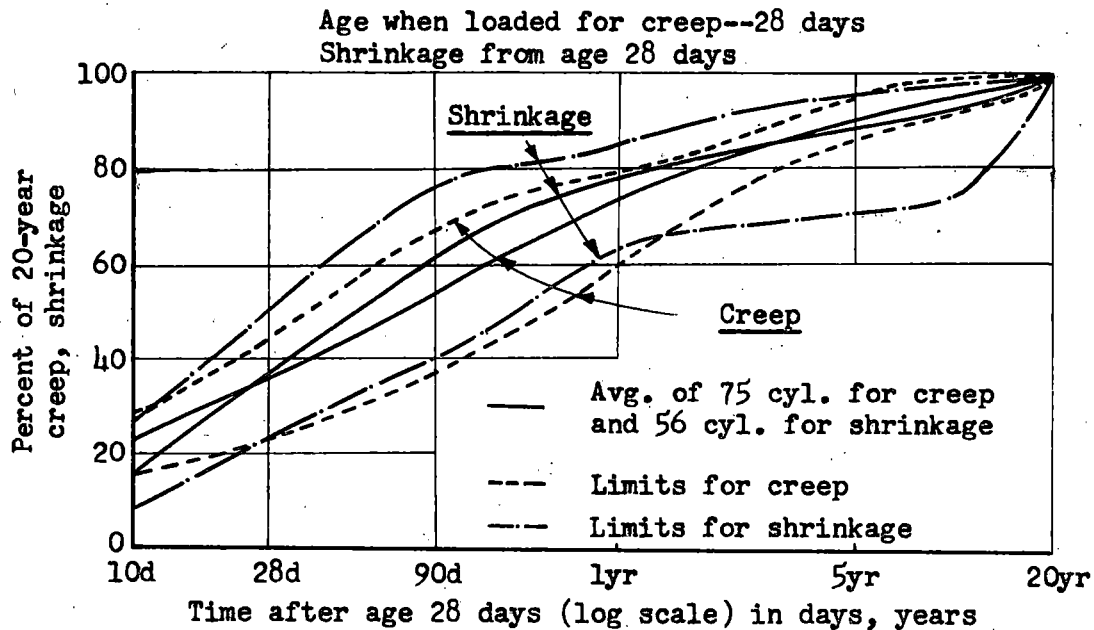


Fig. 5--Creep and shrinkage versus time ratio curves for 20-year normal weight concrete data, from Reference 9

Standard equations--steam cured, 2-3 day loading age, shrinkage from 2-3 days

$$C_t = \frac{t^{0.60}}{11.0 + t^{0.60}} C_u, \quad C_u = 2.10 \quad (9)$$

$$\epsilon_{sh} = \frac{t}{60.0 + t} (\epsilon_{sh})_u, \quad (\epsilon_{sh})_u = 450 \times 10^{-6} \text{ in/in} \quad (10)$$

where t is time in days after loading for creep and time after initial shrinkage is considered.

Standard Eqs. (7) through (10) are plotted in Fig. 4 as a percentage of the ultimate value in each case. The following percentages are noted for the indicated periods after age 7 days for moist cured and 2-3 days for steam cured-- C_t/C_u or $(\epsilon_{sh})/(\epsilon_{sh})_u$ in percent:

	(7)	(8)	(9)	(10)
1 month	41%	56%	Same	33%
3 months	57	79	as	60
4 months	62	84	(7)	67
5 months	65	86		72
6 months	67	89		75
1 year	76	94		86
5 years	89	99		97

The creep and shrinkage curves⁹ in Fig. 5 are based on 20-year data for normal weight concrete with an initial time of 28 days. The results in Figs. 4 and 5 are roughly comparable although some differences are to be found because of the different initial times.

The computed (directly in Eqs. 7 and 8) and measured creep and shrinkage for the moist cured specimens of this project are shown in Figs. 6 and 7.

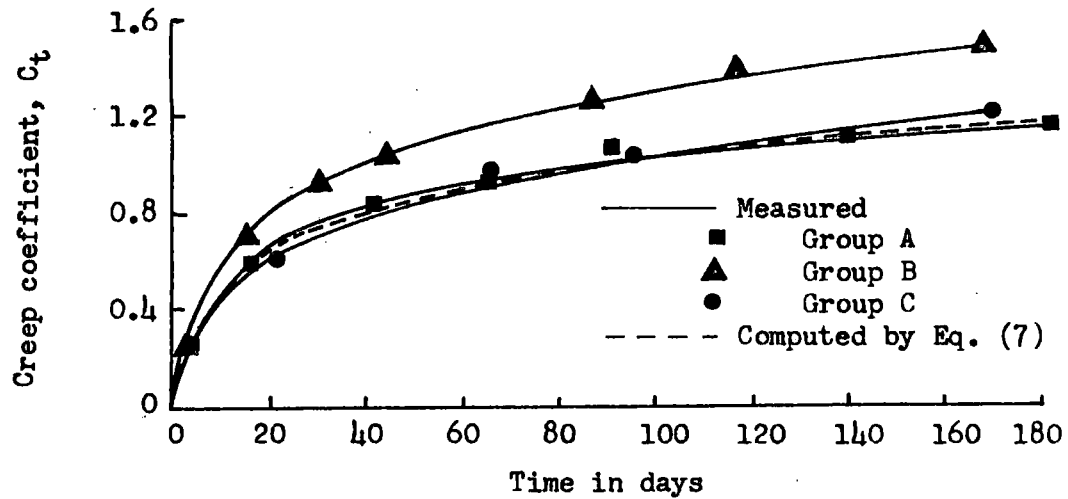


Fig. 6--Measured and computed creep coefficients for the sand-lightweight concrete of Groups A, B, and C--slump less than 3", loaded at age 7 days, average relative humidity 40%, thickness of specimens 6"

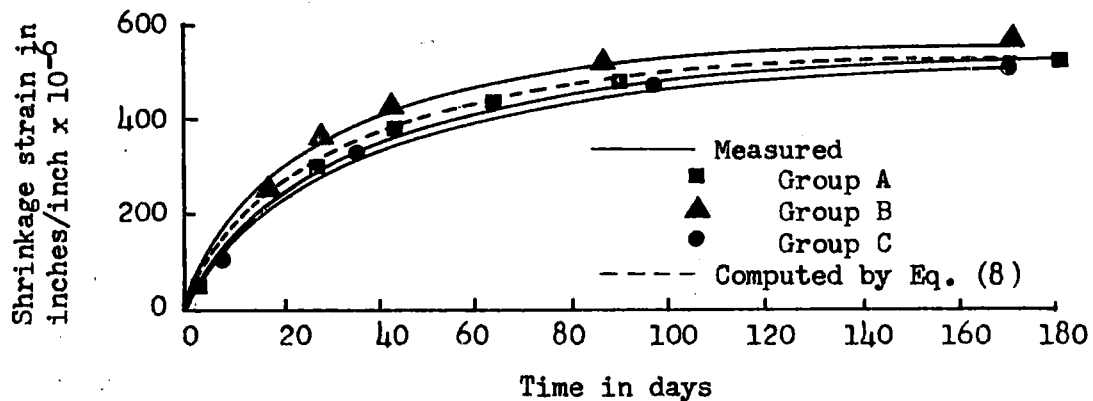


Fig. 7--Measured and computed shrinkage strains for the sand-lightweight concrete of Groups A, B, and C--slump less than 3", shrinkage from age 7 days, average relative humidity 40%, thickness of specimens 6"

Correction factors

All correction factors are applied to ultimate values. However, since creep and shrinkage for any period in Eqs. (7) through (10) are linear functions of the ultimate values, the correction factors in this procedure may be applied to short-term creep and shrinkage as well.

For slumps greater than 3", see Figs. B3 and B4.

For loading ages of other than 7 days for moist cured concrete and 2-3 days for steam cured concrete, see Fig. 2 for the creep correction factor.

For shrinkage considered from other than 7 days for moist cured and 2-3 days for steam cured concrete, determine the differential in Eqs. (8) and (10) for any period starting after this time. For shrinkage of moist cured concrete from 1 day (used to estimate differential shrinkage in composite beams, for example), use Shrinkage C.F. = 1.10.

For other than 40% average relative humidity, assume the following, where H is relative humidity in percent:

Creep--When $H \leq 40\%$, use standard C_t from Eqs. (7) and (9).
 When $H \geq 70\%$, use $0.80 C_t$.
 Interpolate linearly in between $H = 40\%$ and 70% ,
 or When $H = 50\%$, use $0.93 C_t$.
 When $H = 60\%$, use $0.87 C_t$.

Shrinkage--When $H \leq 40\%$, use standard ϵ_{sh} from Eqs. (8) and (10).
 When $H \geq 80\%$, use $0.20 \epsilon_{sh}$.
 Interpolate linearly in between $H = 40\%$ and 80% ,
 or When $H = 50\%$, use $0.80 \epsilon_{sh}$.
 When $H = 60\%$, use $0.60 \epsilon_{sh}$.
 When $H = 70\%$, use $0.40 \epsilon_{sh}$.

For minimum thickness of members greater than 6", see Fig. 3 for the shrinkage correction factor, as a function of length of drying period. This effect is negligible for ultimate values of members whose minimum thickness is less than 15". The effect of member thickness on creep is shown in Fig. B3, and may normally be neglected as explained below.

The following summary and comments refer to other correction factors (shown in Appendix B, Figs. B3 and B4) for creep and shrinkage, which are normally not excessive and tend to offset each other. For design purposes, these may normally be neglected:

Creep

Minimum thickness of member: C.F. = 0.95 for 8", 0.88 for 12".
 Comment--Tends to be offset by slumps greater than 2.5" and cement contents less than 7.5 sacks per cu. yd.
 Slump: C.F. = 0.92 for 2", 1.00 for 2.5", 1.06 for 3", 1.18 for 4", 1.26 for 5". Comment--Tends to be offset by effect of thickness of member.
 Cement content (sacks per cu. yd.): C.F. = 0.98 for 8 sacks, 1.00 for 7.5 sacks, 1.02 for 7 sacks, 1.06 for 6 sacks, 1.16 for 4 sacks. Comment--Small for concrete of say more than 6 sacks, and tends to be offset by effect of thickness.
 Percent fines (by wt.): C.F. = 0.97 for 30-40%, 1.00 for 50%, 1.04 for 60%. Comment--Normally negligible.
 Air content (in %): C.F. = 0.98 for 3-5%, 1.00 for 6%, 1.09 for 8%, 1.42 for 12%. Comment--Negligible for say less than 8% air.

Shrinkage

Slump: C.F. = 0.98 for 2", 1.00 for 2.5", 1.01 for 3", 1.03 for 4", 1.04 for 5". Comment--Normally negligible.
 Cement content (sacks per cu. yd.): C.F. = 1.03 for 8 sacks, 1.00 for 7.5 sacks, 0.97 for 7 sacks, 0.93 for 6 sacks, 0.88 for 4 sacks. Comment--Small for concrete of say more than 6 sacks, and tends to be offset by effect of slump.
 Percent fines (by wt.): C.F. = 0.90 for 40%, 1.00 for 50%, 1.08 for 60%. Comment--May be marginal but normally negligible.
 Air content (in %): C.F. = 0.95 for 4%, 0.97 for 5%, 1.00 for 6%, 1.05 for 8%. Comment--Normally negligible for say up to 8% air.

Reduction factors from References 17 and 33 for 100% sand substitution for fines, as compared to lightweight fines, were: For creep--0 to 30% with 20% used in Reference 33; For shrinkage--3 to 40% with 15% used in Reference 33. These factors are not used herein, since this report refers directly to sand-lightweight concrete data.

In the absence of specific creep and shrinkage data for local aggregates and conditions, the following values will normally be satisfactory for design purposes:

Average-standard-ultimate creep and shrinkage values for normal weight, sand-lightweight, and all-lightweight concrete

For 3" or less slump, $H \leq 40\%$, 7 day loading age for moist cured concrete, or 2-3 day loading age for steam cured concrete:

$$C_u = 2.25$$

For 3" or less slump, $H \leq 40\%$, minimum thickness of member 6" or less,

shrinkage from 7 days for moist cured concrete:

$$(\epsilon_{sh})_u = 650 \times 10^{-6} \text{ in/in}$$

shrinkage from 2-3 days for steam cured concrete:

$$(\epsilon_{sh})_u = 550 \times 10^{-6} \text{ in/in}$$

For other conditions, the same correction factors apply as before.

LOSS OF PRESTRESS

Prediction of prestress loss

Prestressed concrete structures are subjected to relatively high sustained stress for the life of the structure. Under the action of prestress and dead load, large time-dependent deformations occur. In a pretensioned member, the initial prestress is affected by the following:

Elastic shortening

As the prestress is transferred to the concrete, the member shortens, and the prestressed steel shortens with it. The prestress loss due to elastic shortening, in percent, is given by Eq. (11).

$$PL_{el} = (n f_c / f_{si}) 100, \quad f_c = \frac{F_i}{A_t} + \frac{F_i e^2}{I_t} - \frac{M_D e}{I_t} \quad (11)$$

where f_c is the concrete stress at the steel c.g.s. due to prestress and dead load, f_{si} is the initial or tensioning steel stress, and n is the modular ratio at the time of prestressing. Frequently F_o (prestress force after elastic loss), A_g , and I_g are used in Eq. (11) instead of F_i , A_t , and I_t . The results are usually very close.

Concrete creep

Under working loads, concrete creep is approximately proportional to compressive stress. Slight variations in this proportionality (which can be assumed to follow the initial concrete stress-strain curve, according to Reference 11) at the $0.60 f_{ci}$ -stress level, for example, may normally be neglected. For low tensile concrete stress, the rate of concrete creep can be considered the same in tension and compression. The prestress loss due to concrete creep, in percent, is given by Eq. (12).

$$PL_{cp} = PL_{el} C_t \left(1 - 0.5 \frac{\Delta F}{F_o}\right) \quad (12)$$

The expression, $C_t \left(1 - 0.5 \frac{\Delta F}{F_o}\right)$, was used in References 27 and 28 to approximate the creep effect resulting from the variable stress history. Since ΔF refers to the prestress loss that occurs after elastic loss, values assumed herein for this secondary effect (expression in parenthesis) correspond to $\Delta F/F_o = 0.10$, 0.20 , and 0.25 for 1 month, 6 months, and ultimate, respectively.

Concrete shrinkage

While creep strains alter the curvature in a prestressed beam directly, in addition to causing a loss in the initial prestress, shrinkage affects the curvature only indirectly--by causing a loss of prestress. The prestress loss due to shrinkage, in percent, is given by Eq. (13).

$$PL_{sh} = (\epsilon_{sh} E_s / f_{si}) 100 \quad (13)$$

where ϵ_{sh} is the free concrete shrinkage occurring after the time of prestressing, and E_s is the modulus of elasticity of the prestressing steel.

Steel relaxation

Stress relaxation in the steel reduces the initial prestress, thus causing a reduction in curvature and creep. Relaxation in steel is dependent on the type of steel, duration of stressing, initial stress, temperature, prestretching and restretching. It was first thought that relaxation losses were small (2 to 4%) and about 70% of this took place during the first few hours after tensioning. However, it was shown in References 34 and 35 that relaxation losses can be relatively high (especially under high initial stress, which is common in prestressed concrete), and can take place over a long period of time. Based on the work of References 34 and 35, and the tests conducted in this project (discussed in the next section of this report), Eq. (14) is recommended for predicting the prestress loss due to steel relaxation, in percent.

$$PL_r = 1.5 \log_{10} t, \quad \text{Max } PL_r = 7.5\% \text{ at or above } 10^5 \text{ hrs (11.4 yrs).} \quad (14)$$

where t is time after initial stressing in hours. Eq. (14) applies only when f_{si}/f_y is greater than or equal to 0.55, in which f_y is defined as the 0.1%-offset yield strength. This ratio is usually about 0.70 in prestressed concrete structures.

Slab casting in the case of composite beams

When a composite slab is cast on a prestressed concrete member, both elastic and time-dependent effects are produced-- a. the slab dead load causes an elastic change that depends on the age of the concrete at that time; b. due to the sustained slab dead load, creep takes place. Also, the stiffness of the member is increased due to the hardened slab, and this reduces the rate of creep curvature and strain; c. differential shrinkage induces strains that are additive to the slab dead load effect; and d. the prestress in the steel is increased (noticeably so in bridges) due to these effects. For composite beams, Eq. (12) is replaced by Eqs. (15) and (16), and Eqs. (17), (18), and (19) are added for predicting loss of prestress, in percent.

Prestress loss, in percent, due to creep under prestress and precast beam dead load up to the time of slab casting--

$$(PL_{cp})_1 = PL_{el} C_{s2} \left(1 - 0.5 \frac{\Delta F}{F_0}\right) \quad (15)$$

where C_{s2} is the creep coefficient of the precast beam concrete at the time of slab casting. Subscripts 1 and 2 are used herein to refer to the slab (or effect of the slab, such as in Eq. 18 below) and precast beam, respectively.

Same as Eq. (15), except for the period following slab casting--

$$(PL_{cp})_2 = PL_{e1} (C_{t2} - C_{s2}) (1 - 0.5 \frac{\Delta F}{F_o}) (I_2/I_c) \quad (16)$$

where C_{t2} is the creep coefficient of the precast beam concrete at any time after slab casting (including ultimate), and the ratio, I_2/I_c , takes into account the increased stiffness of the member due to the slab.

Prestress gain (elastic), in percent, due to the slab dead load--

$$PG_{e1} = (m f_{cs}/f_{si})100 \quad (17)$$

where f_{cs} is the concrete stress at the steel c.g.s. due to slab dead load (plus diaphragm dead load where applicable), and m is the modular ratio at the time of slab casting. The concrete stress is computed using the precast beam section properties for unshored construction and the composite beam section properties for shored construction.

Prestress gain, in percent, due to creep under slab dead load--

$$PG_{cp} = PG_{e1} C_{t1} (I_2/I_c) \quad (18)$$

where C_{t1} is the creep coefficient for the slab loading, where the age of the precast beam concrete at the time of slab casting is considered.

Prestress gain, in percent, due to differential shrinkage--

$$PG_{ds} = (m f_{cd}/f_{si})100, \quad f_{cd} = \frac{Q y_{cs} e_c}{I_c}, \quad Q = D A_1 E_1 \quad (19)$$

where f_{cd} is the concrete stress at the steel c.g.s. due to differential shrinkage. The differential shrinkage force is applied to the composite section. See the notation for additional descriptions of terms²³.

Theoretical calculation of prestress loss

The total loss of prestress at any time, t , (including the ultimate value) is given by Eq. (20) for non-composite beams and Eq. (21) for composite beams.

Non-composite beams:

$$PL_t = \overset{(11)}{PL_{el}} + \overset{(12)}{PL_{cp}} + \overset{(13)}{PL_{sh}} + \overset{(14)}{PL_r} \quad (20)$$

Composite beams:

$$PL_t = \overset{(11)}{PL_{el}} + \overset{(13)}{PL_{sh}} + \overset{(14)}{PL_r} + \overset{(15)}{(PL_{cp})_1} + \overset{(16)}{(PL_{cp})_2} - \overset{(17)}{PG_{el}} - \overset{(18)}{PG_{cp}} - \overset{(19)}{PG_{ds}} \quad (21)$$

Approximate method for calculating prestress loss

The following approximate method is recommended for estimating the ultimate loss of prestress, in percent, for non-composite and composite structures constructed of normal weight, sand-lightweight, and all-lightweight concrete.

Non-composite beams:

$$PL_u = \left[(n f_c)_{el} + (n f_c C_u)_{cp} + ((\epsilon_{sh})_u E_s)_{sh} + (0.075 f_{si})_r \right] 100/f_{si} \quad (22)$$

Composite beams:

$$PL_u = \left[(n f_c)_{el} + (n f_c \alpha_s C_u)_{cpl} + (n f_c (1 - \alpha_s) C_u (I_2/I_c))_{cp2} + ((\epsilon_{sh})_u E_s)_{sh} + (0.075 f_{si})_r - \underset{\substack{\text{slab} \\ \text{effect}}}{(m f_{cs})_{el}} - \underset{\substack{\text{slab} \\ \text{effect}}}{(\beta_s m f_{cs} C_u) (I_2/I_c)_{\text{time-dep}}} \right] 100/f_{si} \quad (23)$$

where $E_s = 27 \times 10^6$ psi for ASTM A-416 grade (250 K) strands, $E_s = 28 \times 10^6$ psi for 270 K grade strands, I_2 and I_c are the moments of inertia of the precast and composite sections, respectively, α_s refers to the part of the total creep that takes place before slab casting ($\alpha_s = \frac{t^{0.60}}{11 + t^{0.60}}$ herein) and β_s (see Fig. 2) is the creep correction factor for the precast beam concrete age when the slab is cast (under slab dead load).

Compute--

$$f_c = \frac{F_o}{A_g} + \frac{F_o e^2}{I_g} - \frac{M_D e}{I_g} \quad \text{and} \quad f_{cs} = \frac{M_{\text{slab DL}} e}{I_g} \quad \text{for midspan values,}$$

where $F_o = F_i (1 - n p)$, $p = A_s/A_g$. Only the first two terms of f_c apply for end values. $M_{\text{slab DL}}$ includes the diaphragm dead load where applicable. In computing f_{cs} , e and I_g refer to the precast beam section properties for unshored construction and the composite beam section properties for shored construction. For camber calculations, use the midspan loss for 2-point harping (case of bridge girders herein) and an average of the end and midspan loss for 1-point harping and straight tendons (case of laboratory beams herein which used straight tendons).

Substitute the following for normal weight, sand-lightweight, and all lightweight concrete structures (based on 3" or less slump, 70% relative humidity, 7 day loading age and shrinkage from 7 days for moist cured concrete, 2-3 day loading age and shrinkage from 2-3 days for steam cured concrete, no shrinkage correction factor for thickness of members since these refer to ultimate values)--

$$\text{Moist cured: } C_u = .8(2.25) = \underline{1.80}, \quad (sh)_u = .4(650) = \underline{260 \times 10^{-6} \text{ in/in}}$$

$$\text{Steam cured: } C_u = \underline{1.80}, \quad (sh)_u = .4(550) = \underline{220 \times 10^{-6} \text{ in/in}}$$

For the time between prestressing and slab casting (both moist and steam cured)

= 3 weeks,	$\alpha_s = 0.36,$	$\beta_s = 0.65$
1 month,	0.41	0.60
2 months,	0.51	0.45
3 months,	0.57	0.40

Based on $f'_c = 4000$ to 4500 psi for both moist cured (M.C.) and steam cured (S.C.), up to 3-mths- $f'_c = 7090$ to 7420 psi (using Eq. 3) for moist cured and 3-mths- $f'_c = 5120$ to 5750 psi (using Eq. 4) for steam cured, and for both 250 K and 270 K strands; average modular ratios are:

Modular Ratio	Sand-				All-			
	Nor. Wt.		Lt. Wt.		Lt. Wt.		Lt. Wt.	
	(w = 145)		(w = 120)		(w = 100)		(w = 100)	
	M.C.	S.C.	M.C.	S.C.	M.C.	S.C.	M.C.	S.C.
At release of prestress	n =	7.3	7.3	9.8	9.8	12.9	12.9	

For the time between prestressing and slab casting

= 3 weeks,	m =	6.0	6.6	7.9	8.7	10.5	11.6
1 month,		5.8	6.6	7.7	8.7	10.1	11.4
2 months,		5.7	6.5	7.5	8.6	9.9	11.4
3 months,		5.6	6.5	7.4	8.6	9.8	11.3

The results of Eqs. (20) and (21) are shown in Figs. 10 and 11, and Table 2 for the laboratory beams and bridge girders. In the case of the laboratory beams, these results are compared with experimental results in Fig. 10 and Table 2. The ultimate loss of prestress is computed using Eqs. (22) and (23), with both the general parameters defined above and also with the measured parameters for the sand-lightweight concrete of this project. These are compared in Table 2 with the ultimate prestress loss computed by the theoretical method of Eqs. (20) and (21).

Loss of prestress for laboratory beams and bridge girders

Relaxation tests

Relaxation measurements were made for three different diameter 7-wire prestressing strands. The results agreed well with the equation suggested in Reference 34, as can be seen in Fig. 8.

It should be noted, however, that the relaxation of steel stress in a prestressed member takes place under decreasing steel strain (due to shrinkage, creep, etc.), rather than at constant length as in a relaxation test. The loss of prestress due to steel relaxation is also affected by slab casting (level of stress in steel is raised) in the case of composite beams. Due to these effects and the practice of overtensioning to counteract the relaxation that takes place between the time of tensioning and effective bonding of concrete to steel (this practice was assimilated in the laboratory beam tests, where it is noted in Fig. 8 that about 2% relaxation takes place in 24 hours, for example), it is felt that about 75% of the steel relaxation in a constant-length relaxation test should be used in prestressed concrete loss calculations.

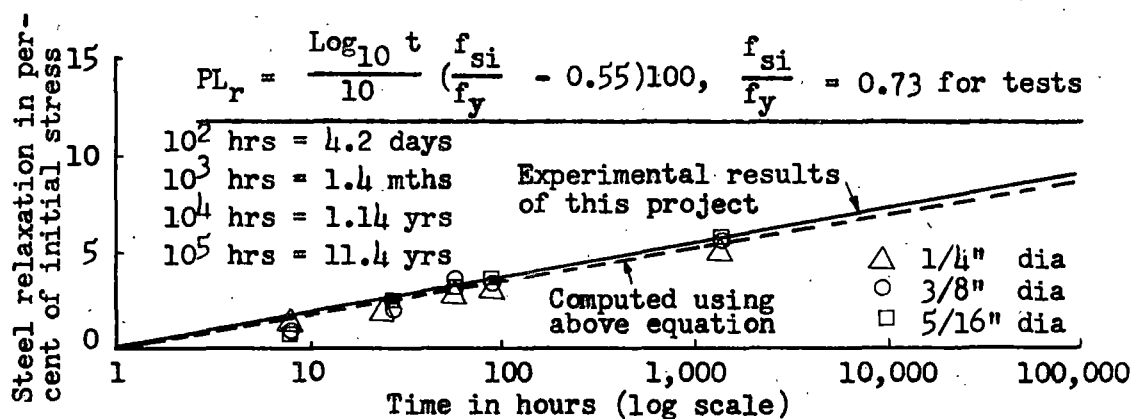
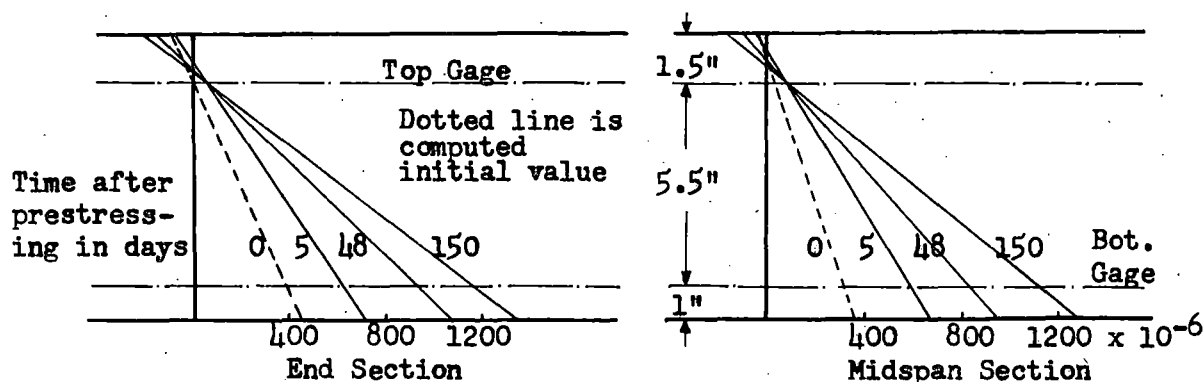


Fig. 8--Measured and computed steel relaxation for relaxation tests



Initial plus time-dependent strain distribution diagrams from concrete strains measured on the sides of the beams

Typical experimental prestress loss determined for end section at 150 days

$f_{si} = 172 \text{ ksi}$, $E_s = 27 \times 10^3 \text{ ksi}$, Observed conc. strain at cgs = $976 \times 10^{-6} \text{ in/in.}$

Loss from meas. strains = $(976 \times 10^{-6})(27 \times 10^3)(100)/172 = 15.3\%$

Inc. in meas. loss due to lateral distribution (det. as 2.5% of 15.3) = 0.4

Meas. loss due to steel relaxation (75% of value from Fig. 8) = 5.3

Total experimental loss of prestress = 21.0%

Fig. 9--Typical measured strain distribution diagrams for the end and midspan sections of Beam B1, and example of experimental prestress loss determined for the end section at 150 days after prestressing

It was concluded in Reference 35, after a careful study, that steel relaxation is probably insignificant beyond 100,000 hours (11.4 yrs), and that this ultimate value might be taken as twice the value at 1000 hours (1.4 mths). The relaxation equation recommended in this report, Eq. (14), is the same time-function ($\log t$) as that of Reference 34, except reduced by 25% in magnitude and incorporating the idea of Reference 35 that the ultimate value be taken as twice that at 1000 hours. This results in an ultimate steel relaxation for prestressed concrete of 7.5%, as shown in Eq. (14).

Experimental and computed loss of prestress for laboratory beams
and computed loss of prestress for bridge girders

The loss of prestress at the end and midspan for the laboratory beams was determined experimentally from the measured concrete strains. However, this measured loss does not include the steel relaxation loss, since steel relaxation is a "stress relaxation at constant length--or nearly so in the case of a prestressed beam" phenomenon. Separate relaxation tests were made and the results shown in Fig. 8 (also see Eq. 14 and discussion). An example of the experimental determination of prestress loss for a typical laboratory beam is shown in Fig. 9.

Experimental and computed loss of prestress versus time curves for the laboratory beams are shown in Fig. 10, and the computed curves for the bridge girders in Fig. 11. The end and midspan values are shown in each case. The separate effects (elastic, creep, shrinkage, relaxation), and how they vary with time, are shown in Fig. 12 for a typical composite laboratory beam and bridge girder.

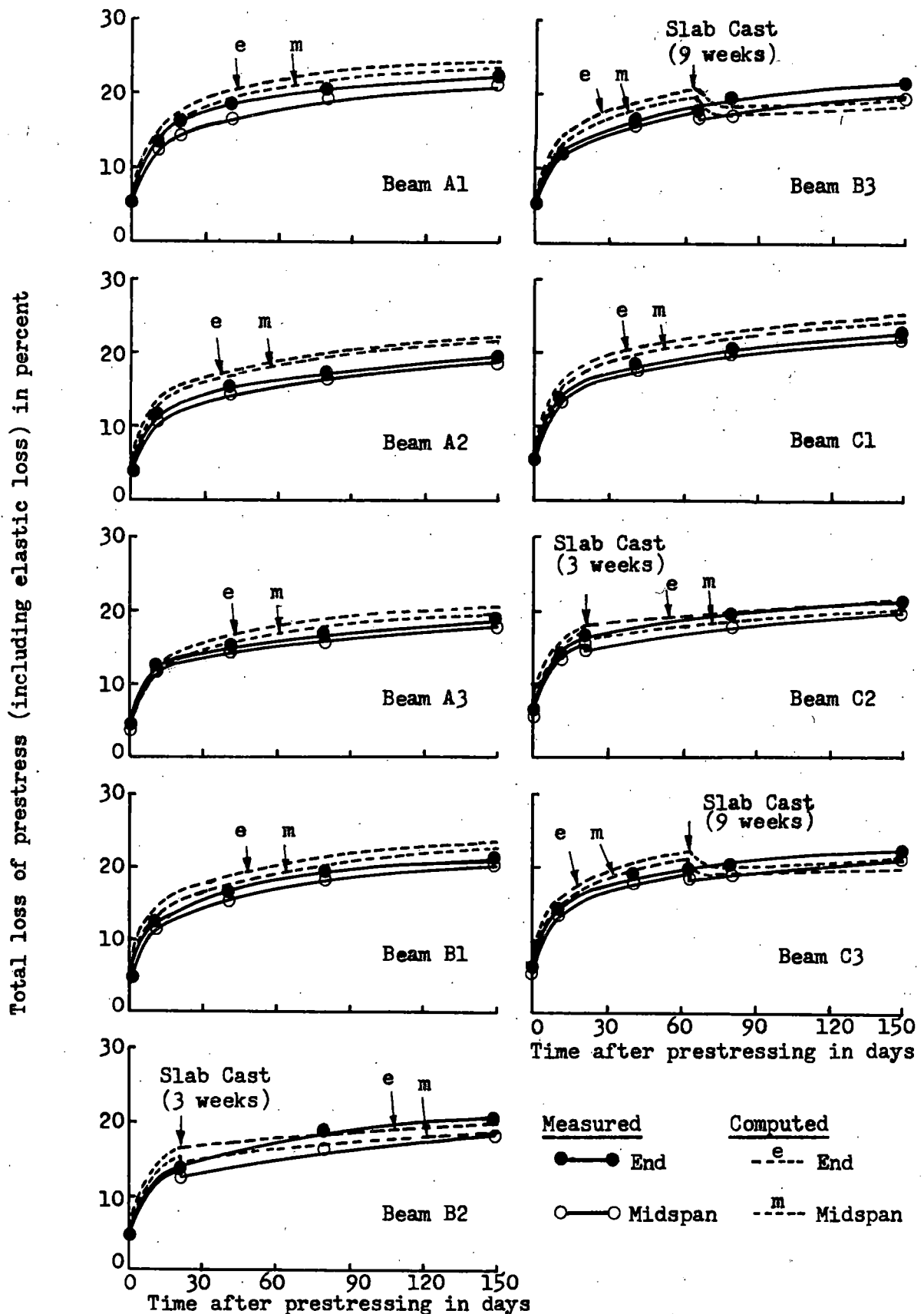
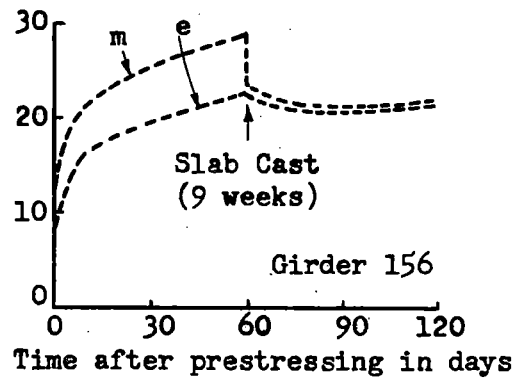
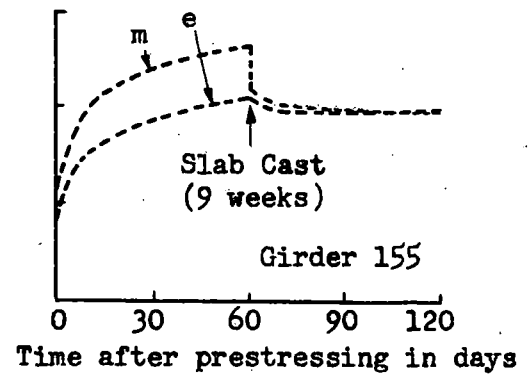
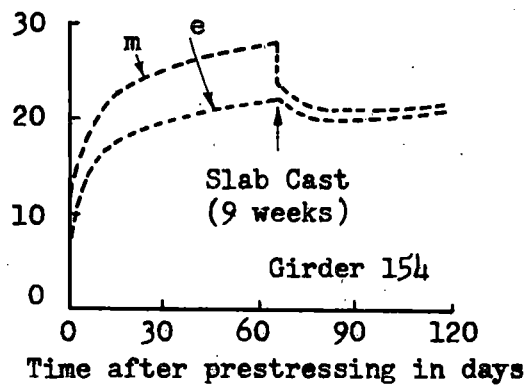
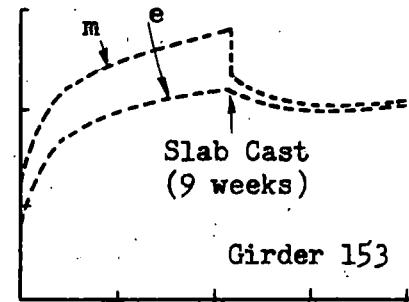
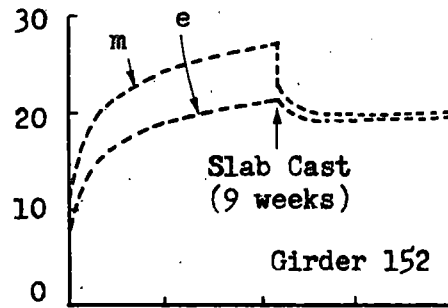


Fig. 10—Measured and computed loss of prestress (by theoretical procedure using Eqs. 20 and 21) for the laboratory beams

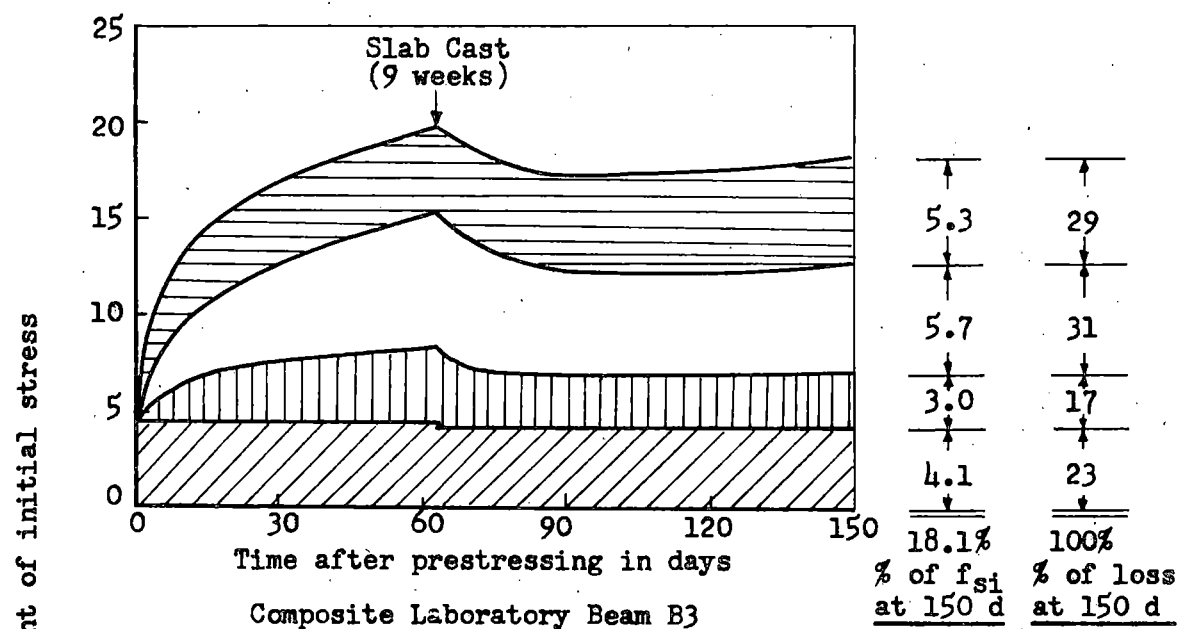
Total loss of prestress (including elastic loss) in percent



--- e --- End

--- m --- Midspan

Fig. 11--Computed loss of prestress (by theoretical procedure using Eq. 21) for the bridge girders



Elastic Loss
 Creep Loss
 Shrinkage Loss
 Relaxation Loss

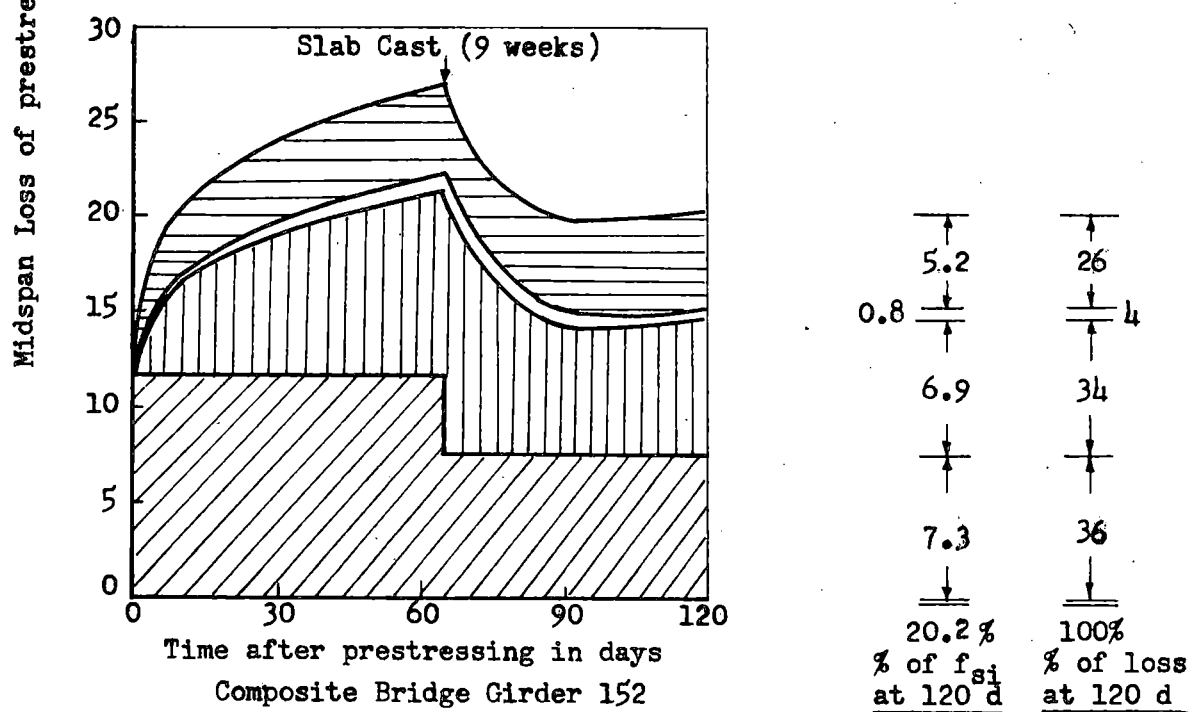


Fig. 12--Computed loss of prestress, showing separate effects, for typical composite lab. beam and bridge girder (by theoretical procedure--Eq. 21) versus time. Diff. shrinkage is included in shrinkage part

The experimental and computed loss of prestress for the laboratory beams and computed loss for the bridge girders are shown in Table 2 at the time just prior to slab casting, and at 150 days for the beams and 120 days for the girders. The computed ultimate values are also tabulated in Table 2 using: the theoretical Eqs. (20) and (21) with experimental parameters determined for the sand-lightweight concrete of this project, the approximate Eqs. (22) and (23) with the experimental parameters of this project, and Eqs. (22) and (23) with general parameters given for normal weight, sand-lightweight, and all-lightweight concrete. In the general procedure, the same creep and shrinkage factors are suggested for all three concretes, with different modular ratios for each. The calculations in this report are for sand-lightweight concrete only. The computed losses using the experimental parameters are shown by terms in Table 3 for the theoretical Eqs. (20) and (21), and in Table 4 for the approximate Eqs. (22) and (23).

Based on the results of Figs. 10, 11, 12, and Tables 2, 3, 4, the following observations are made:

1. The experimental loss of prestress for the laboratory beams was slightly lower than the computed loss for the non-composite beams (possibly due to the use of creep data based on a uniform stress distribution rather than non-uniform), and about the same for the composite beams. This can be seen in Fig. 10 and Table 2 where the ratio of computed to experimental loss of prestress at 150 days varied from 0.91 to 1.16. Based on these comparisons and the camber comparisons in the next chapter, both the theoretical and approximate methods for computing loss of prestress are thought to be satisfactory.

¹TABLE 2--EXPERIMENTAL AND COMPUTED LOSS OF PRESTRESS FOR LABORATORY BEAMS AND COMPUTED LOSS OF PRESTRESS FOR BRIDGE GIRDERS

Beam No.	2Time Bet. Pres. and Slab Cast	3Experi- mental Loss at 150 days		Computed Loss Just Before Slab Cast		Computed Loss by Theoretical Eqs. 20, 21, with exp. param., at 150 d. for Lab. B. and 120 d. for Br.Gr.				4Computed Ultimate Loss					
										Theor. Eqs. 20, 21 with exp. param.		Approx.Eqs. 22, 23 with exp. param.		Approx.Eqs. 22, 23 with gen. param.	
		End	Mid	Mid	Ratio	End	Ratio	Mid	Ratio	End	Mid	End	Mid	End	Mid
	Laboratory Beams														
A1	--	22.7	21.8	--	--	24.7	1.09	23.8	1.09	30.9	29.8	32.1	30.8	4--	4--
A2	--	19.9	18.0	--	--	22.5	1.13	21.5	1.16	27.7	27.0	29.1	27.9	--	--
A3	--	18.9	18.0	--	--	20.6	1.09	19.7	1.10	25.8	24.7	26.6	25.3	--	--
B1	--	21.0	20.1	--	--	23.5	1.12	22.5	1.12	29.4	28.2	30.5	29.1	--	--
B2	21 d.	20.8	18.2	15.6	1.14	19.9	0.96	18.6	1.02	24.9	23.4	26.6	25.0	--	--
B3	63 d.	21.2	19.9	19.8	1.10	19.5	0.92	18.1	0.91	24.5	22.9	27.6	26.0	--	--
C1	--	22.7	22.1	--	--	25.4	1.12	24.5	1.11	31.0	30.7	33.2	31.2	--	--
C2	21 d.	21.6	20.0	17.3	1.10	21.6	1.00	20.3	1.01	26.9	25.4	28.5	27.0	--	--
C3	63 d.	22.7	21.8	21.7	1.13	21.3	0.94	20.0	0.92	26.6	25.2	29.7	28.2	--	--
	Bridge Girders														
152	65 d.	--	--	26.9	--	20.0	--	20.2	--	26.7	27.6	27.7	29.2	30.7	32.3
153	65 d.	--	--	28.0	--	20.7	--	21.1	--	27.5	28.7	28.6	29.9	30.7	32.3
154	65 d.	--	--	27.8	--	20.5	--	21.1	--	27.3	28.5	28.5	29.7	30.7	32.3
155	60 d.	--	--	26.6	--	19.9	--	19.8	--	26.5	27.1	27.6	28.8	30.7	32.3
156	60 d.	--	--	28.3	--	20.9	--	21.3	--	27.7	28.9	28.8	30.1	30.7	32.3

¹All losses are expressed in percent of initial stress. The ratios are: Computed/Experimental.

²The laboratory beams and bridge girders were prestressed at age 7 days and 2-3 days, respectively. The 150 day and 120 day times in the table refer to times after prestressing.

³See Fig. 9 for example of experimental prestress loss determination.

⁴The general parameters suggested in the report refer to field conditions and design concrete properties. Hence, only the bridge girder values are included in the last two columns. See Footnote 2, Table 3 and Footnote 2, Table 4 for a description of the experimental parameters.

^{1,2}TABLE 3--COMPUTED ULTIMATE LOSS OF PRESTRESS AT MIDSPAN, BY TERMS, FOR THE LABORATORY BEAMS AND BRIDGE GIRDERS, USING THE THEORETICAL EQS. (20) AND (21) WITH EXPERIMENTAL PARAMETERS

Beam No.	El. Loss Eq. 11	Shrink Loss Eq. 13	Relax Loss Eq. 14	Creep Loss Before Slab Cast, Eq. 12 or 15	Creep Loss After Slab Cast, Eq. 16	El. Gain Due to Slab Eq. 17	Creep Gain Due to Slab Eq. 18	Gain Due to Diff. Shrink Eq. 19	Total Loss, Eqs. 20, 21
<u>Laboratory Beams</u>									
A1	5.2	9.2	7.5	7.9	--	--	--	--	29.8
A2	4.1	9.2	7.5	6.2	--	--	--	--	27.0
A3	3.2	9.2	7.5	4.8	--	--	--	--	24.7
B1	4.5	9.2	7.5	6.9	--	--	--	--	28.1
B2	4.5	9.2	7.5	2.5	1.4	-0.4	-0.2	-1.1	23.4
B3	4.5	9.2	7.5	3.6	1.0	-0.4	-0.1	-2.4	22.9
C1	5.5	9.2	7.5	8.5	--	--	--	--	30.7
C2	5.5	9.2	7.5	3.1	1.7	-0.4	-0.2	-1.0	25.4
C3	5.5	9.2	7.5	4.4	1.3	-0.4	-0.1	-2.3	25.1
<u>Bridge Girders</u>									
152	11.5	2.6	7.5	9.0	2.7	-4.2	-1.1	-0.4	27.6
153	12.1	2.6	7.5	9.4	2.8	-4.2	-1.1	-0.4	28.7
154	12.0	2.6	7.5	9.3	2.8	-4.2	-1.1	-0.4	28.5
155	11.5	2.6	7.5	8.8	2.7	-4.4	-1.1	-0.5	27.1
156	12.4	2.6	7.5	9.5	2.9	-4.4	-1.1	-0.5	28.9

¹All losses are expressed in percent of initial stress.

²The experimental parameters used in the above calculations are shown in Table 1 (elastic and strength properties) and elsewhere in this report for the sand-lightweight concrete of this project. The correction factors given in the report are used, where appropriate, for relative humidity and age of loading. The creep and shrinkage factors used are:

	<u>Laboratory Beams</u>	<u>Bridge Girders</u>
Precast beam creep:	$C_u = 1.75$	$C_u = 1.68$
Precast beam shrinkage ($\times 10^{-6}$ in/in): $(\epsilon_{sh})_u = 590$		$(\epsilon_{sh})_u = 180$
Slab shrinkage---used in calculating differential shrinkage ($\times 10^{-6}$ in/in): $(\epsilon_{sh})_u = 430$		$(\epsilon_{sh})_u = 120$

^{1,2}TABLE 4--COMPUTED ULTIMATE LOSS OF PRESTRESS AT MIDSPAN, BY TERMS,
FOR THE LABORATORY BEAMS AND BRIDGE GIRDERS, USING THE
APPROXIMATE EQS. (22) AND (23) WITH EXPERIMENTAL PARAMETERS

Beam No.	El. Loss Term	Shrink Loss Term	Relax Loss Term	Creep Loss Before Slab Cast Term	Creep Loss After Slab Cast Term	El. Gain Due to Slab Term	Time-Dep Gain Due to Slab Term	Total Loss, Eqs. 22, 23
<u>Laboratory Beams</u>								
A1	5.1	9.2	7.5	9.0	--	--	--	30.8
A2	4.1	9.2	7.5	7.1	--	--	--	27.9
A3	3.1	9.2	7.5	5.5	--	--	--	25.3
B1	4.5	9.2	7.5	7.9	--	--	--	29.1
B2	4.5	9.2	7.5	2.8	1.6	-0.4	-0.2	25.0
B3	4.5	9.2	7.5	4.1	1.2	-0.4	-0.1	26.0
C1	5.5	9.2	7.5	9.6	--	--	--	31.8
C2	5.5	9.2	7.5	3.4	2.0	-0.4	-0.2	27.0
C3	5.5	9.2	7.5	5.0	1.5	-0.4	-0.1	28.2
<u>Bridge Girders</u>								
152	11.4	2.6	7.5	10.0	3.0	-4.2	-1.1	29.2
153	11.7	2.6	7.5	10.3	3.1	-4.2	-1.1	29.9
154	11.6	2.6	7.5	10.2	3.1	-4.2	-1.1	29.7
155	11.4	2.6	7.5	9.8	3.0	-4.4	-1.1	28.8
156	12.0	2.6	7.5	10.4	3.1	-4.4	-1.1	30.1

¹All losses are expressed in percent of initial stress.

²Footnote 2 of Table 3 also applies to this table, except that differential shrinkage is not included in the approximate method; hence the slab shrinkage is not used in the approximate method.

2. The 3 beams of Group A and the beams of Groups B and C demonstrate the fact that higher concrete stress levels result in higher prestress losses, for the same initial steel stress, due to higher initial concrete strains (see Table 2 and A2).

3. Slab casting causes an elastic prestress gain and a time-dependent gain due to creep and differential shrinkage. Creep loss under prestress and precast beam dead load is also reduced by the effect of the composite section. This gain (or reduction in prestress loss) is smaller for the laboratory beams than the bridge girders, due to their relative sizes. A comparison of composite beams B2, B3 and C2, C3 with non-composite beams B1, and C1, respectively, in Table 2 indicates that the composite slab reduces the ultimate loss by 4.1% to 5.5% (from 30.7% to 25.2% = 5.5%, for example). The corresponding reduction in ultimate loss of prestress for the bridge girders due to the composite slab was about 12% (as $41\% - 29\% = 12\%$). These effects can be seen in various ways in Figs. 10, 11, 12, and Tables 2, 3, 4.

4. The effect of the 3 week and 9 week slab casting schedules had only a small effect on loss of prestress for the laboratory beams (less than 1% loss as shown in Table 2). The computed loss was slightly less, not greater as might be expected, for the 9 week slabs than the 3 week slabs, because of the high differential shrinkage effect in the low humidity laboratory ($H = 40\%$). This was verified by the experimental data at 5 months after prestressing as well.

As expected, the computed ultimate loss of prestress (using theoretical Eq. 21 with experimental parameters) for the bridge girders of this project when considering a 3 week slab, as compared to the actual 9 week slab, was about $2\frac{1}{2}\%$ lower at midspan (prestress loss $2\frac{1}{2}\%$ lower for 3

week slab). The results of Eq. (21) for the five bridge girders are as follows:

Girder No.	Computed ultimate loss of prestress by Eq. (21), with experimental parameters, in % of initial stress			
	3 Week Slab		*9 Week Slab	
	End	Midspan	End	Midspan
152	25.4	25.1	26.7	27.6
153	26.2	26.2	27.5	28.7
154	26.0	26.0	27.3	28.5
155	25.4	24.9	26.5	27.1
156	26.5	26.6	27.7	28.9

*These values from Table 2

5. As shown in Figs. 10 and 11, and Table 2, the difference in the end and midspan loss of prestress was quite small for the laboratory beams, and relatively large for the bridge girders before slab casting. After slab casting, the loss of prestress in the bridge girders was only slightly different at end and midspan.

In the case of the laboratory beams (straight tendon profile), the midspan stress at the steel c.g.s. level was only slightly lower than at the beam end, due to the relatively small precast beam dead load stress at midspan. The midspan stress due to the laboratory beam slabs was also relatively small. Hence, the loss of prestress for the laboratory beams was slightly greater at the end than at midspan (Fig. 10). For the bridge girders (2-point harping profile), the midspan stress at the steel c.g.s. level is considerably higher at midspan than at the end of the girder (2700 psi as compared to 1900 psi). The greater midspan eccentricity in the harped bridge girders more than offsets the dead load stress. The result is a considerably higher prestress loss at midspan than at the end before the deck slab is cast (Fig. 11). The composite deck serves to

greatly reduce this midspan loss, so that the end and midspan values are nearly the same after slab casting (Fig. 11 and Table 2).

6. For a typical composite bridge girder, it is shown in Fig. 12 that the separate effects contribute to the loss of prestress in the following proportions at 120 days after prestressing: elastic--7.3% loss or 36% of total loss, creep--6.9% loss or 34% of total loss, shrinkage--0.8% loss or 4% of total loss (this includes differential shrinkage which causes a gain in prestress), and steel relaxation--5.2% loss or 26% of total loss. Similar values for a typical composite laboratory beam, and how these values vary with time for both laboratory beams and bridge girders, can also be seen in Fig. 12.

7. The computed loss of prestress using the theoretical and approximate equations with experimental parameters of this project, and the approximate equations with general parameters given in this report, are tabulated in Table 2. In noting the results by these three methods in that order, the prestress loss values differ by about 1% to 3% between methods (as 27.6% to 29.2% to 32.3%), in the order one would expect; that is, with the general approximate method on the high side, etc. The ultimate loss of prestress for both the laboratory beams and bridge girders of this project is of the order of 25% to 30% for these sand-lightweight prestressed concrete structures. The 4 and 5 month (after prestressing) loss of prestress for both was about 19% to 23% (Figs. 10 and 11, and Table 2).

8. The prestress loss due to creep of the precast beam concrete after slab casting is greatly reduced because of the increased stiffness of the member. The effect of shrinkage loss and differential shrinkage gain is much more pronounced in the case of the laboratory beams than the bridge

girders because of the much higher shrinkage in the lower humidity laboratory (40% versus 70%). These effects, as well as the elastic and time-dependent (due to creep under slab dead load) prestress gain, can be seen in Fig. 12 and the term-by-term tabulations in Tables 3 and 4, except that differential shrinkage is not included in the approximate method shown in Table 4.

CAMBER

Prediction of camber

The theoretical and approximate methods in this report for predicting camber of non-composite and composite prestressed concrete beams are extensions of the work in References 21, 27, and 28.

Theoretical calculation of camber

Non-composite beams:

$$\Delta_t = + \overbrace{(\Delta_i)_{F_0}}^{(1)} - \overbrace{(\Delta_i)_{DL}}^{(2)} + \overbrace{\left[-\frac{\Delta F}{F_0} + \left(1 - \frac{\Delta F}{2F_0}\right) C_t \right]}^{(3)} \overbrace{(\Delta_i)_{F_0}}^{(4)} - C_t \overbrace{(\Delta_i)_{DL}}^{(4)} \quad (24)$$

where: (1) is the initial camber due to the initial prestress force after elastic loss, F_0 . See Appendix C for common cases of prestress moment diagrams with formulas for computing camber, $(\Delta_i)_{F_0}$.

(2) is the initial dead load deflection of the beam. $(\Delta_i)_{DL} = K M L^2 / E_{ci} I_g$. See notation for K and M formulas.

(3) is the creep (time-dependent) camber of the beam due to the prestress force. This expression includes the effects of creep and loss of prestress; that is, the creep effect under variable stress. ΔF refers to the total loss at any time minus the elastic loss.

(4) is the dead load creep deflection of the beam.

It is noted that the term $\Delta F / F_0$ refers to the steel stress or force after elastic loss, and the prestress loss in percent, PL, (as used herein) refers to the tensioning stress or force. The two are related as:

$$\frac{\Delta F}{F_0} = \frac{1}{100} (PL_{total} - PL_{el}) \frac{f_{si}}{f_0} \quad (25)$$

Eq. (25) can be very closely approximated by Eq. (26)

$$\frac{\Delta F}{F_0} = \frac{1}{100} (PL_{total} - PL_{el}) \frac{1}{1 - n p} \quad (26)$$

where n is the modular ratio at the time of prestressing, and $p = A_s/A_g$.

Unshored composite beams:

$$\begin{aligned}
 \Delta_t = & \overbrace{+(\Delta_i)_{F_0}}^{(1)} - \overbrace{(\Delta_i)_2}^{(2)} + \overbrace{\left[-\frac{\Delta F_s}{F_0} + \left(1 - \frac{\Delta F_s}{2 F_0}\right) C_{s2} \right] (\Delta_i)_{F_0}}^{(3)} \\
 & + \overbrace{\left[-\frac{\Delta F_t}{F_0} + \left(1 - \frac{\Delta F_t}{2 F_0}\right) (C_{t2} - C_{s2}) \right] (\Delta_i)_{F_0} \frac{I_2}{I_c}}^{(4)} - \overbrace{C_{s2} (\Delta_i)_2}^{(5)} \\
 & - \overbrace{(C_{t2} - C_{s2}) (\Delta_i)_2 \frac{I_2}{I_c}}^{(6)} - \overbrace{(\Delta_i)_1}^{(7)} - \overbrace{C_{t1} (\Delta_i)_1 \frac{I_2}{I_c}}^{(8)} - \overbrace{\frac{Q y_{cs} L^2}{8 E_c I_c}}^{(9)} \quad (27)
 \end{aligned}$$

where: (1) is the initial camber due to the initial prestress force after elastic loss, F_0 . See Appendix C for common cases of prestress moment diagrams with formulas for computing camber, $(\Delta_i)_{F_0}$.

(2) is the initial dead load deflection of the precast beam.
 $(\Delta_i)_2 = K_2 M_2 L^2 / E_{ci} I_g$. See notation for K and M formulas.

(3) is the creep (time-dependent) camber of the precast beam up to the time of slab casting. ΔF_s refers to the total loss at the time of slab casting minus the initial elastic loss that occurred at the time of prestressing. C_{s2} is the creep coefficient of the precast beam concrete at the time of slab casting.

(4) is the creep camber of the composite beam for any period following slab casting. ΔF_t refers to the total loss at any time following slab casting (including ultimate) minus the initial elastic loss that occurred at the time of prestressing. C_{t2} is the creep coefficient of the precast beam concrete at any time after slab casting (including ultimate).

(5) is the creep deflection of the precast beam up to the time of slab casting due to the precast beam dead load.

(6) is the creep deflection of the composite beam for any period following slab casting due to the precast beam dead load.

- (7) is the initial deflection of the precast beam under slab dead load. $(\Delta_i)_1 = K_1 M_1 L^2 / E_c I_g$. See notation for K and M formulas. When diaphragms are used, add to $(\Delta_i)_1$: $(\Delta_i)_{1D} = \frac{M_{1D}}{E_c I_g} \left(\frac{L^2}{8} - \frac{a^2}{6} \right)$,

where M_{1D} is the moment between diaphragms, and a is $L/4$, $L/3$, etc., for 2 symmetrical diaphragms at quarter points, third points, etc., respectively.

- (8) is the creep deflection of the composite beam due to the slab dead load. C_{t1} is the creep coefficient for the slab loading, where the age of the precast beam concrete at the time of slab casting is considered.

- (9) is the deflection due to differential shrinkage.

Shored composite beams:

$$\Delta_t = \text{Eq. (27), with Terms (7) and (8) modified as follows:} \quad (28)$$

- (7) is the initial deflection of the composite beam under slab dead load. $(\Delta_i)_1 = K_1 M_1 L^2 / E_c I_c$. For this case, the composite moment of inertia, I_c , is used.
- (8) is the creep deflection of the composite beam due to the slab dead load = $C_{t1} (\Delta_i)_1$. The composite-section effect is already included in Term (7).

It is suggested that the 28-day moduli of elasticity for both slab and precast beam concretes be used in computing the composite moment of inertia, I_c , for Eqs. (27) and (28).

Approximate method for calculating camber

The following approximate method is recommended for estimating the ultimate camber of non-composite and composite structures constructed of normal weight, sand-lightweight, and all-lightweight concrete. All needed material parameters are defined with Eqs. (22) and (23) in the loss of prestress chapter. Other notation in Eqs. (29) through (31) is the same as defined with Eqs. (24), (27), and (28). In addition, ΔF_u refers to the total ultimate loss of prestress minus the initial elastic loss that occurred at the time of prestressing.

The following loss of prestress ratios at the time of slab casting and ultimate are suggested for use in the approximate Eqs. (29), (30), and (31) for normal weight, sand-lightweight, and all-lightweight concrete structures:

$\Delta F_s/F_o$ for 3 wks to 1 mth between prestressing and slab casting =
0.11 for Nor. Wt., 0.13 for Sand Lt. Wt., 0.15 for All Lt. Wt.

$\Delta F_s/F_o$ for 2 to 3 mths between prestressing and slab casting =
0.15 for Nor. Wt., 0.18 for Sand Lt. Wt., 0.21 for All Lt. Wt.

$\Delta F_u/F_o = 0.22$ for Nor. Wt., 0.25 for Sand Lt. Wt., 0.29 for All Lt. Wt.

Note that these are defined as the total loss (at slab casting and ultimate) minus the initial elastic loss divided by the prestress force after elastic loss.

Non-composite beams:

$$\Delta_u = + \overbrace{(\Delta_i)_{F_o}}^{(1)} - \overbrace{(\Delta_i)_{DL}}^{(2)} + \overbrace{\left[-\frac{\Delta F_u}{F_o} + \left(1 - \frac{\Delta F_u}{2 F_o}\right) C_u \right] (\Delta_i)_{F_o}}^{(3)} - \overbrace{C_u (\Delta_i)_{DL}}^{(4)} \quad (29)$$

Unshored composite beams:

$$\begin{aligned} \Delta_u = & + \overbrace{(\Delta_i)_{F_o}}^{(1)} - \overbrace{(\Delta_i)_2}^{(2)} + \overbrace{\left[-\frac{\Delta F_s}{F_o} + \left(1 - \frac{\Delta F_s}{2 F_o}\right) \alpha_s C_u \right] (\Delta_i)_{F_o}}^{(3)} \\ & + \overbrace{\left[-\frac{\Delta F_u}{F_o} + \left(1 - \frac{\Delta F_u}{2 F_o}\right) (1 - \alpha_s) C_u \right] (\Delta_i)_{F_o} \frac{I_2}{I_c}}^{(4)} - \overbrace{\alpha_s C_u (\Delta_i)_2}^{(5)} \\ & - \overbrace{(1 - \alpha_s) C_u (\Delta_i)_2 \frac{I_2}{I_c}}^{(6)} - \overbrace{(\Delta_i)_1}^{(7)} - \overbrace{\beta_s C_u (\Delta_i)_1 \frac{I_2}{I_c}}^{(8)} - \overbrace{*D.S.}^{(9)} \quad (30) \end{aligned}$$

*See discussion following Eq. (31) for treatment of differential shrinkage.

Shored composite beams:

$$\Delta_u = \text{Eq. (30), except that the composite moment of inertia is used in Term (7) to compute } (\Delta_i)_1, \text{ and the ratio, } I_2/I_c, \text{ is eliminated in Term (8).} \quad (31)$$

The terms in the approximate Eqs. (29) and (30) correspond to the same terms in the theoretical Eqs. (24) and (27). When shrinkage is expected to be relatively high (such as in low humidity regions), the differential shrinkage term (Term 9) in Eq. (27) should be included in Eq. (30); otherwise Term (9) may be omitted in Eq. (30). Term (9) was omitted in the case of the bridge girders ($H = 70\%$) and included in the case of the laboratory beams ($H = 40\%$) in the approximate method (Eq. 30) in this report. This effect can be seen in the term-by-term solutions in Tables 6 and 7.

The solution of Eq. (30) or (31) for camber of composite beams requires only the calculation of $(\Delta_i)_{F_0}$, $(\Delta_i)_2$, and $(\Delta_i)_1$ -- see formulas for these as defined with Eq. (27) or (28) -- in addition to the section properties and prestress force, $F_0 = F_i(1 - \frac{n f_c}{f_{si}})$, where f_c is determined as suggested following Eq. (23). All other parameters are given here and with Eqs. (22) and (23). The same is true for non-composite beams and Eq. (29), -- $(\Delta_i)_{F_0}$ and $(\Delta_i)_{DL}$ being defined with Eq. (24).

Measured and computed midspan camber for laboratory beams and bridge girders

Measured and computed midspan camber versus time curves for the laboratory beams and bridge girders are shown in Figs. 13 and 14. These camber values are tabulated and compared in Table 5 at release of prestress (initial camber), just before slab casting (3 and 9 weeks for the laboratory beams and 9 weeks for the bridge girders after prestressing), and at 5 months for the laboratory beams and 4 months for the bridge girders after prestressing. The computed ultimate values are also shown in Table 5 for: the theoretical Eqs. (24) and (27) with experimental parameters determined for the sand-lightweight concrete of this project, the approximate Eqs. (29) and (30) with experimental parameters of this project, and Eqs. (29) and (30) with general parameters given for normal weight, sand-lightweight, and all-lightweight concrete.

In the general procedure, the same creep and shrinkage factors are suggested for all three concretes, but with different prestress loss ratios $\Delta F_s/F_0$ and $\Delta F_u/F_0$ for each. The calculations in this report are for sand-lightweight concrete only. The computed camber values using the experimental parameters are shown by terms in Table 6 for the theoretical Eqs. (24) and (27), and in Table 7 for the approximate Eqs. (29) and (30).

Based on the results of Figs. 13, 14, and Tables 5, 6, 7, the following observations are made:

1. The computed initial camber compared very well in most cases with the measured initial camber for both the laboratory beams and bridge girders. The ratio of computed to measured camber varied in Table 5 from 0.93 to 1.10, except for one ratio which was 1.20.

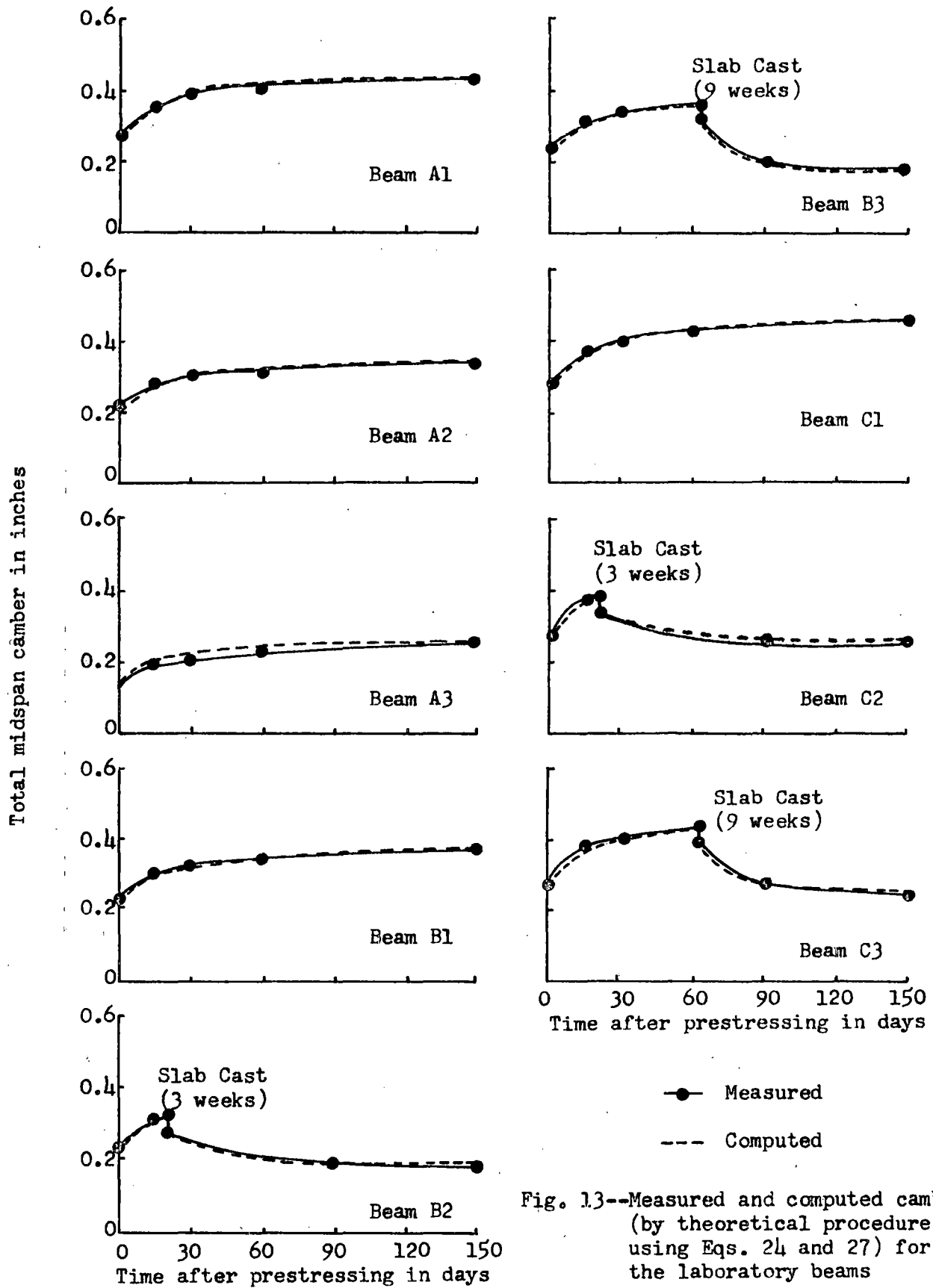


Fig. 13--Measured and computed camber (by theoretical procedure using Eqs. 24 and 27) for the laboratory beams

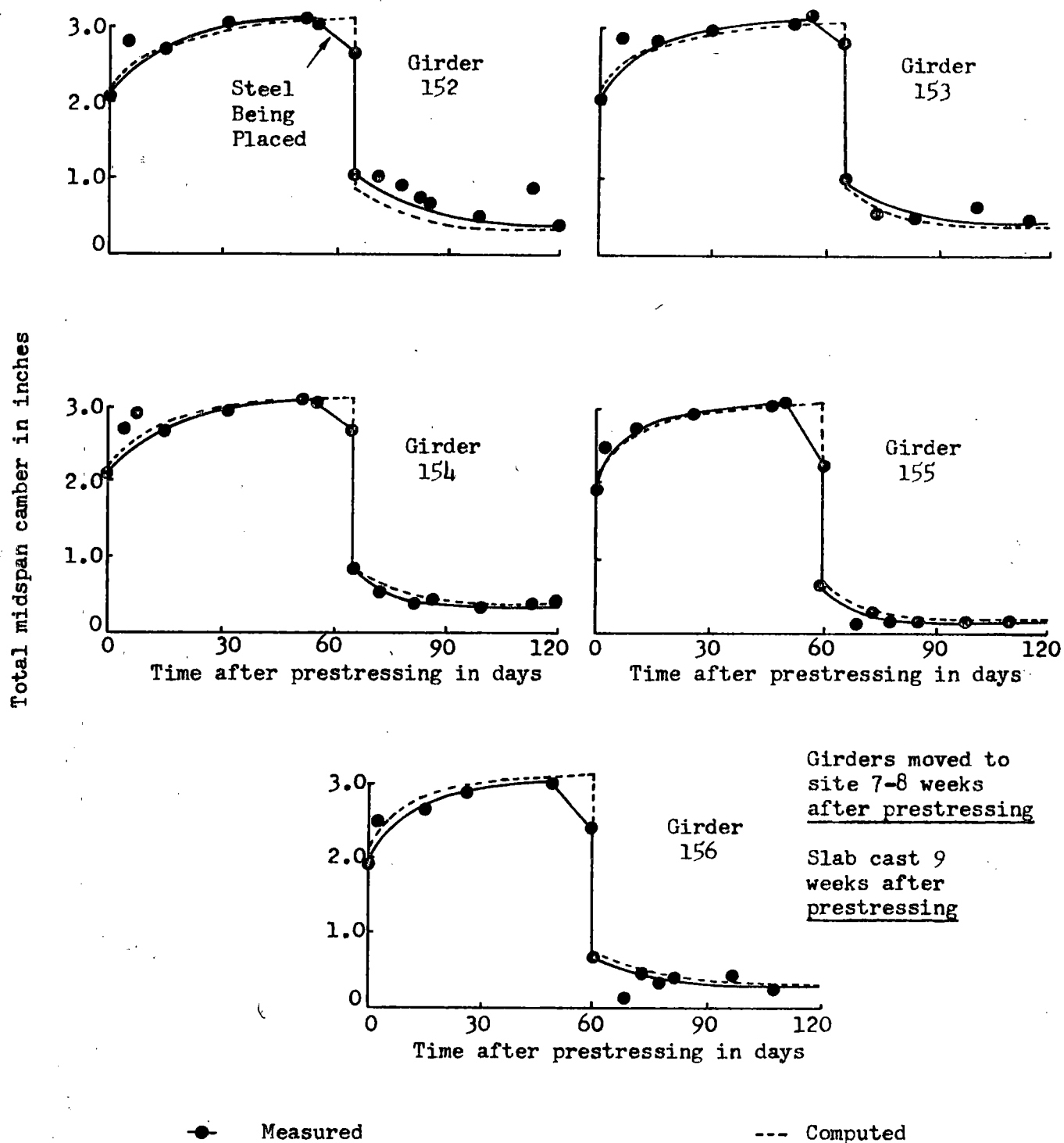


Fig. 14--Measured and computed camber (by theoretical procedure using Eq. 27) for the bridge girders

¹TABLE 5--MEASURED AND COMPUTED MIDSPAN CAMBER FOR LABORATORY BEAMS AND BRIDGE GIRDERS

Beam No.	Initial Camber			2Time Bet. Pres. and Slab Cast	Camber Just Before Slab Cast			Computed Camber by Theoretical Eqs. 24, 27, with exp. param., at 150 d. for Lab. B. and 120 d. for Br.Gr.			3Computed Ultimate Camber		
	Meas.	Comp.	Ratio		Meas.	Comp.	Ratio	Meas.	Comp.	Ratio	Theor. Eqs. 24, 27 with exp. param.	Approx.Eqs. 29, 30 with exp. param.	Approx.Eqs. 29, 30 with gen. param.
Laboratory Beams													
A1	0.27	0.25	0.93	--	--	--	--	0.44	0.44	1.00	0.54	0.56	3--
A2	0.20	0.21	1.05	--	--	--	--	0.34	0.34	1.00	0.43	0.44	--
A3	Bad D.	0.14	--	--	--	--	--	0.26	0.26	1.00	0.31	0.32	--
B1	0.22	0.22	1.00	--	--	--	--	0.38	0.37	0.97	0.47	0.48	--
B2	0.23	0.22	0.96	21 d.	0.32	0.31	0.97	0.18	0.20	1.11	0.22	0.23	--
B3	0.23	0.22	0.96	63 d.	0.36	0.35	0.97	0.18	0.17	0.95	0.18	0.19	--
C1	0.27	0.27	1.00	--	--	--	--	0.47	0.46	0.98	0.58	0.60	--
C2	0.27	0.27	1.00	21 d.	0.39	0.38	0.97	0.26	0.28	1.08	0.31	0.32	--
C3	0.27	0.27	1.00	63 d.	0.44	0.43	0.98	0.26	0.25	0.96	0.28	0.30	--
Bridge Girders													
152	2.05	2.10	1.02	65 d.	3.10	3.03	0.98	0.40	0.33	0.83	40.41	40.51	0.66
153	2.05	2.18	1.06	65 d.	3.15	3.10	0.98	0.45	0.39	0.87	0.47	0.60	0.66
154	2.10	2.19	1.04	65 d.	3.15	3.12	0.99	0.40	0.41	1.03	0.51	0.64	0.66
155	1.90	2.10	1.10	60 d.	3.06	3.01	0.98	0.20	0.21	1.05	0.33	0.43	0.66
156	1.85	2.23	1.20	60 d.	3.00	3.12	1.04	0.31	0.31	1.00	0.42	0.53	0.66

¹All camber values are in inches. The ratios are: Computed/Measured.

²The laboratory beams and bridge girders were prestressed at age 7 days and 2-3 days, respectively. The 150 day and 120 day times in the table refer to times after prestressing.

³The general parameters suggested in the report refer to field conditions and design concrete properties. Hence, only the bridge girder values are included in the last column. See Footnote 2, Table 3 and Footnote 2, Table 4 for a description of the experimental parameters.

⁴The differential shrinkage term of 0.10" (omitted in the approximate method for bridge girders) represents the principal difference in these computed results between the theoretical and approximate methods.

^{1,2}TABLE 6--COMPUTED ULTIMATE MIDSPAN CAMBER, BY TERMS, FOR THE LABORATORY BEAMS AND BRIDGE GIRDERS, USING THE THEORETICAL EQS. (24) AND (27) WITH EXPERIMENTAL PARAMETERS

Beam No.	Initial Camber Due to Prestr.	Initial Defl. Due to Beam DL	Creep Camber Up to Slab Cast	DL Defl. to Slab Cast	Creep Up Camber After Slab Cast	Bm.DL Defl. After Slab Cast	El. Defl. Due to Slab DL	Creep Defl. Due to Slab DL	Defl. Due to Shrink age	Total Camber, Eqs. 24,27
	Term 1	Term 2	Term 3	Term 4	Term 5	Term 6	Term 7	Term 8	Term 9	
<u>Laboratory Beams</u>										
A1	0.30	-0.05	0.38	-0.09	--	--	--	--	--	0.54
A2	0.24	-0.05	0.33	-0.09	--	--	--	--	--	0.43
A3	0.19	-0.05	0.26	-0.09	--	--	--	--	--	0.31
B1	0.27	-0.05	0.35	-0.09	--	--	--	--	--	0.47
B2	0.27	-0.05	0.12	-0.03	0.07	-0.02	-0.05	-0.02	-0.07	0.22
B3	0.27	-0.05	0.18	-0.05	0.04	-0.02	-0.04	-0.01	-0.14	0.18
C1	0.32	-0.05	0.40	-0.09	--	--	--	--	--	0.58
C2	0.32	-0.05	0.14	-0.03	0.08	-0.02	-0.05	-0.02	-0.06	0.31
C3	0.32	-0.05	0.21	-0.05	0.06	-0.02	-0.04	-0.01	-0.14	0.28
<u>Bridge Girders</u>										
152	3.72	-1.62	2.36	-1.43	0.67	-0.43	-2.21	-0.55	-0.10	0.41
153	3.88	-1.70	2.42	-1.50	0.68	-0.45	-2.21	-0.55	-0.10	0.47
154	3.87	-1.68	2.42	-1.49	0.69	-0.44	-2.21	-0.55	-0.10	0.51
155	3.72	-1.62	2.31	-1.40	0.68	-0.42	-2.30	-0.55	-0.09	0.33
156	3.97	-1.74	2.40	-1.51	0.70	-0.46	-2.30	-0.55	-0.09	0.42

¹All table values are in inches.

²See Footnote 2, Table 3 for a description of the experimental parameters.

^{1,2}TABLE 7--COMPUTED ULTIMATE MIDSPAN CAMBER, BY TERMS, FOR THE LABORATORY BEAMS AND BRIDGE GIRDERS, USING THE APPROXIMATE EQS. (29) AND (30) WITH EXPERIMENTAL PARAMETERS

Beam No.	Initial Camber Due to Prestr.	Initial Defl. Due to Beam DL	Creep Camber Up to Slab Cast	DL Creep Defl. to Slab Cast	Creep Camber After Slab Cast	Bm.DL Defl. After Slab Cast	El. Defl. Due to Slab DL	Creep Defl. Due to Slab DL	3Defl. Due to Diff. Shrink age	Total Camber, Eqs. 29,30
	Term 1	Term 2	Term 3	Term 4	Term 5	Term 6	Term 7	Term 8	Term 9	
Laboratory Beams										
A1	0.31	-0.05	0.39	-0.09	--	--	--	--	--	0.56
A2	0.25	-0.05	0.33	-0.09	--	--	--	--	--	0.44
A3	0.20	-0.05	0.26	-0.09	--	--	--	--	--	0.32
B1	0.27	-0.05	0.35	-0.09	--	--	--	--	--	0.48
B2	0.27	-0.05	0.13	-0.03	0.07	-0.02	-0.05	-0.02	-0.07	0.23
B3	0.27	-0.05	0.19	-0.05	0.04	-0.02	-0.04	-0.01	-0.14	0.19
C1	0.33	-0.05	0.41	-0.09	--	--	--	--	--	0.60
C2	0.33	-0.05	0.15	-0.03	0.07	-0.02	-0.05	-0.02	-0.06	0.32
C3	0.33	-0.05	0.22	-0.05	0.06	-0.02	-0.04	-0.01	-0.14	0.30
Bridge Girders										
152	3.72	-1.62	2.36	-1.43	0.67	-0.43	-2.21	-0.55	--	0.51
153	3.90	-1.70	2.43	-1.50	0.68	-0.45	-2.21	-0.55	--	0.60
154	3.89	-1.68	2.43	-1.49	0.69	-0.44	-2.21	-0.55	--	0.64
155	3.72	-1.62	2.32	-1.40	0.68	-0.42	-2.30	-0.55	--	0.43
156	3.97	-1.74	2.42	-1.51	0.70	-0.46	-2.30	-0.55	--	0.53

¹All table values are in inches.

²See Footnote 2, Table 3 and Footnote 2, Table 4 for a description of the experimental parameters.

³As explained in the discussion of Eq. (30), the differential shrinkage term (Term 9) is omitted in the case of the bridge girders ($H = 70\%$) and included in the case of the laboratory beams ($H = 40\%$) in the approximate method for composite beams.

2. The computed and measured camber versus time curves for the laboratory beams in Fig. 13 and the bridge girders in Fig. 14 are also in good agreement. This can be seen in Table 5 where the ratio of computed to measured camber just before slab casting, in the case of the composite beams, varied from 0.97 to 1.04. This ratio for the laboratory beams at 5 months after prestressing was 0.95 to 1.11; and for the bridge girders at 4 months after prestressing was 0.83 to 1.05. Based on these comparisons and the prestress loss comparisons in the previous chapter, both the theoretical and approximate methods for computing camber are thought to be satisfactory.

3. Slab casting causes an elastic deflection and a time-dependent deflection due to creep and differential shrinkage. The creep camber due to prestress and precast beam dead load are also reduced by the effect of the composite section after the slab has hardened. This deflection after slab casting (or reduction in camber) is smaller for the laboratory beams than the bridge girders because of their relative sizes. A comparison of composite beams B2, B3 and C2, C3 with non-composite beams B1 and C1 in Table 5 indicates that the composite slab reduces the ultimate camber by 52% to 62% (from 0.47" to 0.18" or 62%, for example). In the case of the bridge girders, it can be seen in Fig. 14 that the camber curves have nearly leveled off at about 3.0" (Table 5) just before slab casting. After slab casting and up to ultimate, the camber values in Table 5 are about 0.3" to 0.5". This is a reduction of from 3.0" to say 0.4" or about 87%. The principal reason for the obviously large slab effect in reducing ultimate camber was differential shrinkage for the laboratory beams (high shrinkage in the low humidity laboratory--H = 40%), and elastic deflection (plus creep to a lesser extent).

under slab dead load for the bridge girders. The effect of the slab can be seen in various ways in Figs. 13, 14, and Tables 5, 6, 7.

4. The effect of the 3 week and 9 week slab casting schedules was smaller than expected for the laboratory beams. This was due to the offsetting effects of greater creep camber for the 9 week slabs and greater deflection due to differential shrinkage for the 9 week slabs. The greater creep camber for a later slab casting schedule is due to the fact that the later slab allows more creep camber to take place before the slab is cast (see Tables 6 and 7). In the case of differential shrinkage, the later the slab is cast, the greater is the differential in shrinkage between slab and precast beam. Also, the differential shrinkage for the laboratory beams was relatively high in the low humidity laboratory. In fact, the computed ultimate camber of the laboratory beams was slightly less, not greater, for the 9 week slabs than the 3 week slabs, because of the high differential shrinkage effect. This was verified by the experimental data at 5 months after prestressing as well (see Table 5).

As expected, the computed ultimate camber (using theoretical Eq. 27 with experimental parameters) for the bridge girders of this project when considering a 3 week slab, as compared to the actual 9 week slab, was reduced about 0.3". The ultimate camber by Eq. (27) varied from $-0.04"$ to $0.16"$, avg. 0.09" for a 3 week slab; and from $0.33"$ to $0.51"$ (Table 2), avg. 0.43" for the 9 week slab.

5. The computed ultimate camber using the theoretical and approximate equations with the experimental parameters of this project, and the approximate equations with general parameters given in this study, are tabulated in Table 5. In noting the results by these three methods in

that order, the values differ by relatively small amounts in the order one would expect; that is, with the general approximate method on the high side, etc. The difference between the results by the first two methods was from 0.10" to 0.13" (as $0.64" - 0.51" = 0.13"$), and between the last two methods was from 0.02" to 0.23" (as $0.66" - 0.64" = 0.02"$). The approximate general method was applied to the bridge girders only, as explained in Footnote 3, Table 5. These are thought to be quite reasonable results.

In the case of the bridge girders, the difference between the results by the theoretical and approximate methods with experimental parameters was about 0.10" for each girder (Table 5). This difference is a direct result of the differential shrinkage term (which is 0.10" in Table 6) being omitted in the approximate method for the bridge girders, as explained in Eq. (30). The difference between the results by the approximate method using both experimental and general parameters is due primarily to the slightly larger general creep coefficient specified, and the slightly lower modulus of elasticity used in the general method (design concrete strength slightly lower than actual measured concrete strength). The computed ultimate camber of the bridge girders by the approximate method using experimental parameters (including the measured strength and shrinkage properties, and $C_u = 1.68$) varied from 0.43" to 0.64"; and by the approximate method using general parameters (including general design strength and shrinkage properties, and $C_u = 1.80$) was 0.66". These camber values are also considered quite satisfactory (see Table 5).

6. The camber due to creep of the precast beam concrete after slab casting is greatly reduced because of the increased stiffness of the

member, the lower strain and hence creep level, and the effect of differential shrinkage. These effects, as well as the initial and time-dependent camber and deflection due to the different loads, time periods, and material responses involved, can be seen in the term-by-term tabulations in Tables 6 and 7; except that differential shrinkage is included in the results by the approximate method for the laboratory beams only in Table 7, as explained in Eq. (30).

It is noted that a differential shrinkage term is excluded in the approximate loss of prestress Eq. (23) and, in the case of low ambient humidity conditions--high shrinkage, included in the approximate camber Eq. (30). As can be seen in Tables 3 for loss of prestress and 6, 7 for camber, differential shrinkage has a relatively more significant effect on camber than loss of prestress.

7. Repeated attempts were made to describe a simple method for computing initial plus time-dependent (total) camber of composite beams that could be made to fit the experimental data reasonably well. However, it was concluded that it is necessary to include all 8 terms (omitting differential shrinkage in the case of field structures, unless humidity is low) of Eqs. (30) and (31) in order to incorporate all significant effects in the prediction of residual camber of composite prestressed concrete flexural members. This can be seen in the term-by-term tabulations in Tables 6 and 7 where each of the 8 terms for the bridge girders varied in magnitude from 0.42" to 3.97". It appears to the authors that any simpler method that does not include all of these effects could easily lead to very erroneous results. The results in the sample calculation chapter by one rough approximate method tends to bear this out.

SAMPLE CALCULATIONS

The following numerical substitutions for ultimate loss of prestress at midspan, using the approximate Eq. (23), and ultimate midspan camber, using the approximate Eq. (30), are made for the sand-lightweight, steam cured bridge girders of this project (and using the general design parameters suggested herein).

Parameters in Eqs. (23) and (30) and locations in report

Span = 86 ft, girder spacing = 7 ft, given.

$n = 9.8$, for steam cured sand-lightweight concrete with material properties as defined following Eq. (23).

$f_c = 2405$ psi, from equation following Eq. (23). Also using $F_1 = 867$ kips, e (at midspan) = 14.5 in, $A_s = 4.59$ in², $A_g = 520$ in², $p = 0.00883$, $I_g = 108,500$ in⁴, $M_D = 411$ ft-k (precast beam), F_o (for f_c calculation only) = 793 kips.

$C_u = 1.80$, $(\epsilon_{sh})_u = 220 \times 10^{-6}$ in/in, from info. following Eq. (23).

$E_s = 28 \times 10^6$ psi, as suggested for 270 K grade strand following Eq. (23).

$f_{si} = 190,000$ psi, from discussion preceding Table 1.

$\alpha_s = 0.51$, from information following Eq. (23) for 2 month period between prestressing and slab casting.

$I_2 = I_g$ (above) = 108,500 in⁴, $I_c = 339,000$ in⁴, in which the slab width is reduced by a factor of $E_{slab}/E_{stem} = 3.25/3.41 = 0.95$ (see E's below).

$f_{cs} = 1006$ psi, from equation following Eq. (23), using M_{slab} DL (including diaphragm moment at midspan) = 630 ft-k, I_g is the same as above for unshored construction in computing f_{cs} .

$\beta_s = 0.45$, from information following Eq. (23) for 2 month period between prestressing and slab casting.

$m = 8.6$, for steam cured sand-lightweight concrete with material properties as defined following Eq. (23).

method with experimental parameters of this project.

Eq. (30):

$$\Delta_u = \begin{matrix} (1) & (2) & (3) & (4) & (5) & (6) & (7) & (8) \\ 4.10 & - 1.76 & + 2.68 & + 0.68 & - 1.62 & - 0.50 & - 2.32 & - 0.60 \end{matrix} = 0.66"$$

This term-by-term solution by the approximate method with general design parameters compares closely with the term-by-term results in Table 7 by the approximate method with experimental parameters of this project.

Approximate solution sometimes used

$$\Delta_u = \Delta_i + \Delta_i C_u I_2/I_c, \text{ where } \Delta_i = (\Delta_i)_{F_0} - (\Delta_i)_2 - (\Delta_i)_1$$

Substituting the above parameters here:

$$\Delta_i = 4.10 - 1.76 - 2.32 = 0.02"$$

$$\begin{aligned} \Delta_u &= 0.02 + (0.02)(1.80)(108,500/339,000) \\ &= 0.02 + 0.01 = 0.03". \end{aligned}$$

This answer of 0.03" is seen to be considerably different from the result above of 0.66". This illustrates one of the conclusions in this report that rough approximate methods for predicting camber of composite beams, which do not take into account all of the effects represented by the 8 terms in Eq. (30), can easily lead to very erroneous results.

SUMMARY AND CONCLUSIONS

Methods and parameters are presented for predicting loss of prestress and camber of non-composite and composite prestressed concrete structures. Detailed observations pertaining to the results in this project are outlined at the end of the prestress loss and camber chapters, and only the principal conclusions are mentioned here.

The data and calculations in this report refer to sand-lightweight concrete laboratory and bridge members, although parameters are given for normal weight and all-lightweight concrete as well. In the general procedure recommended for computing prestress loss and camber, the same creep and shrinkage factors are suggested for all three concretes; the primary differences being found in the modular ratios specified (see information following Eq. 23) and the precast beam dead load.

In all cases, the methods presented for predicting material behavior and structural response were in quite good agreement with the experimental data.

The following is a summary of topics included in the report:

1. Equations for predicting the time variation and ultimate values for concrete strength, modulus of elasticity, creep, and shrinkage of both moist cured and steam cured sand-lightweight concrete. Parameters related to these properties are also suggested for normal weight and all-lightweight concrete.

2. A discussion of the principal variables affecting creep and shrinkage is included in Appendix B and condensed for design usage in the text. Specific design parameters are suggested for normal conditions of

field structures in Iowa (such as relative humidity, etc.). Correction factors for other conditions are also given.

3. Both theoretical and approximate methods with experimental parameters (for sand-lightweight concrete) of this project, and approximate methods with general parameters (for different weight concretes) given in this report, for calculating loss of prestress and camber of non-composite and composite prestressed concrete structures. The time-variation in prestress loss and camber, up to ultimate, is included. Separate steel relaxation tests were made and incorporated in the prediction methods.

The principal conclusions of this study are the following:

1. The prediction methods presented in this report appear to be satisfactory (Figs. 1, 6, 7, 10, 13, 14, and Tables 2 and 5). See Observation 1 in the loss of prestress chapter and Observations 1 and 2 in the camber chapter for numerical comparisons between computed and measured values.

2. The loss of prestress for the sand-lightweight concrete bridge girders was of the order of 20% to 21% at 4 months after prestressing and 27% to 29% ultimately (see Fig. 11 and Table 2). It seems clear that loss percentages for bridges under similar conditions using normal weight concrete will normally be somewhat smaller than these; and using all-lightweight concrete will normally be somewhat higher than these (perhaps of the order of 35% to 40%). Without the deck slab, the losses for the same stress level would be even higher. Higher losses for the lighter concretes are due primarily to the lower modulus of elasticity of these concretes (higher elastic strains for a given stress level), and not, necessarily, to greater creep and shrinkage behavior.

3. The composite slab reduces the ultimate loss of prestress of the bridge girders about 12% (as 41% - 29% = 12%). It can be seen in Fig. 14 that the camber curves have nearly levelled off at about 3.0" (see Table 5) just before slab casting. After slab casting and up to ultimate, the camber

values and in Table 5 are about 0.3" to 0.5". This is a reduction of from 3.0" to say 0.4" or about 87%. The main reason for the obviously large slab effect in reducing the ultimate loss of prestress and ultimate camber was the elastic deformation (plus creep to a lesser extent) under slab dead load.

4.-The ultimate loss of prestress for the bridge girders when considering a 3 week slab (slab cast 3 weeks after prestressing), as compared to the actual 9 week slab, was about 2 $\frac{1}{2}$ % lower at midspan (prestress loss was 2 $\frac{1}{2}$ % less for the 3 week slab). See Observation 4 in the loss of prestress chapter for details. As noted in Observation 4 of the camber chapter, the ultimate camber of the bridge girders when considering a 3 week slab, as compared to the actual 9 week slab, was reduced about 0.3" (ultimate camber averaged 0.09" for a 3 week slab and 0.43" for the 9 week slab). These results serve to point out the beneficial effect, from the standpoint of loss of prestress and camber, of casting the deck slab as early as possible.

5. It appears to be necessary to include all 8 terms (omitting differential shrinkage in the case of field structures, unless humidity is low) of Eqs. (30) and (31) in order to incorporate all significant effects in the prediction of residual camber of unshored and shored composite flexural members. This can be seen in the term-by-term tabulations in Tables 6 and 7 where each of the 8 terms for the bridge girders varied in magnitude from 0.42" to 3.97". A simpler method, that does not include all of these effects, may lead to very erroneous results. The result in the sample calculation chapter by one rough approximate method tends to bear this out (ultimate camber of 0.66" by Eq. 30 and 0.03" by rough method). A similar conclusion, but to a lesser degree, is made with regard to the loss of prestress and the 7 terms of Eq. (23) for composite members (see Tables 3 and 4).

6. The computed loss of prestress and camber using the theoretical and approximate equations with experimental parameters (for sand-lightweight concrete) of this project, and the approximate equations with general parameters (for different weight concretes) given in this report, are tabulated in Tables 2 and 5. In noting the results by these three methods in that order, the values differ by relatively small amounts in the order one would expect; that is, with the general approximate method on the high side, etc. The ultimate prestress loss values differed by about 1% to 3% between methods (as 27.6% to 29.2% to 32.3% in Table 2). In the case of the ultimate camber results in Table 5, the difference between the first two methods was from 0.10" to 0.13" (as $0.64" - 0.51" = 0.13"$), and between the last two methods was from 0.02" to 0.23" (as $0.66" - 0.64" = 0.02"$). The computed ultimate camber of the bridge girders by the approximate method using experimental parameters (including the measured strength and shrinkage properties, and $C_u = 1.68$) varied from 0.43" to 0.64"; and by the approximate method using general parameters (including general design strength and shrinkage properties, and $C_u = 1.80$) was 0.66". These are thought to be quite reasonable results.

7. It is noted that a differential shrinkage term is excluded in the approximate loss of prestress Eq. (23) and, in the case of low ambient humidity conditions--high shrinkage, included in the approximate camber Eq. (30). In computing camber by the approximate method, the differential shrinkage term was included for the laboratory beams ($H = 40\%$) and not included for the bridge girders ($H = 70\%$). As can be seen in Tables 3 for loss of prestress and 6, 7 for camber, differential shrinkage has a relatively more significant effect on camber than loss of prestress.

REFERENCES

1. Davis, R., "A Summary of Investigation of Volume Changes in Cement Mortars and Concrete Produced by Causes Other Than Stress," ASTM, Proceedings V. 30, Part I, 1930, pp. 668-685.
2. Carlson, R. W., "Drying Shrinkage of Concrete as Affected by Many Factors," ASTM, Proceedings V. 38, Part II, 1938, pp. 419-440.
3. Hveem, F. N., and Tremper, B., "Some Factors Influencing the Shrinkage of Concrete," ACI Journal, Proceedings V. 53, No. 8, Feb. 1957, pp. 781-802.
4. ACI Committee 435, "Deflections of Reinforced Concrete Flexural Members," ACI Journal, Proceedings V. 63, No. 6, June 1966, pp. 637-674.
5. Lorman, W. R., "The Theory of Concrete Creep," ASTM, Proceedings V. 40, 1940, pp. 1082-1102.
6. McHenry, Douglas, "A New Aspect of Creep in Concrete and Its Application to Design," ASTM, Proceedings V. 43, 1943, pp. 1969-1984.
7. Neville, A. M., "Theories of Creep in Concrete," ACI Journal, Proceedings V. 52, No. 1, Sept. 1955, pp. 47-60.
8. Ross, A. D., "Creep of Concrete Under Variable Stress," ACI Journal, Proceedings V. 54, No. 9, Mar. 1958, pp. 739-758.
9. Troxell, G. E.; Raphael, J. M.; and Davis, R. E., "Long Time Creep and Shrinkage Tests of Plain and Reinforced Concrete," ASTM, Proceedings V. 58, 1958, pp. 1-20.
10. Kesler, C. E., and Ali, I., "Mechanisms of Creep," Symposium on Creep of Concrete," ACI Special Publication No. 9, 1964, pp. 35-63.
11. Meyers, B. L.; Slate, F. O.; and Winter, G., "Time-Dependent Deformation and Microcracking of Plain Concrete," ACI Journal, Proceedings V. 66, No. 1, Jan. 1969, pp.
12. Meyers, B. L., and Neville, A. M., "Creep of Concrete: Influencing Factors and Prediction," Symposium on Creep of Concrete, ACI Special Publication No. 9, 1964, pp. 1-33.
13. Pauw, A., and Chai, J. W., "Creep and Creep Recovery for Plain Concrete," Missouri Cooperative Highway Research Programme, Report No. 67-8.
14. Hansen, T. C., and Mattock, A. H., "Influence of Size and Shape of Member on Shrinkage and Creep of Concrete," ACI Journal, Proceedings V. 63, No. 2, Feb. 1966, pp. 267-290.

15. Jones, T. R.; Hirsch, T. J.; and Stephenson, H. K., "The Physical Properties of Structural Quality Lightweight Aggregate Concrete," Texas Transportation Institute, Texas A & M University, College Station, Texas, August 1959, pp. 1-46.
16. ACI Committee 213, "Guide for Structural Lightweight Aggregate Concrete," ACI Journal, Proceedings V. 64, No. 8, Aug. 1967, pp. 433-470.
17. Pfeifer, D. W., "Sand Replacement in Structural Lightweight Concrete--Creep and Shrinkage Studies," ACI Journal, Proceedings V. 65, No. 2, Feb. 1968, pp. 131-142.
18. Finsterwalder, Ulrick, "Ergebnisse von Kriech und Schwindmessungen an Spannbetonbauwerken," Beton und Stahlbetonbau (Berlin), V. 53, No. 5, May 1958, pp. 136-144.
19. Lofroos, W. N., and Ozell, A. M., "The Apparent Modulus of Elasticity of Prestressed Concrete Beams Under Different Stress Levels," Prestressed Concrete Institute Journal, V. 4, No. 2, Sept. 1959, pp. 23-47.
20. Mattock, Alan H., "Precast-Prestressed Concrete Bridges; 5. Creep and Shrinkage Studies," Journal, Research and Development Laboratories, Portland Cement Association, V. 3, No. 2, May 1961, pp. 32-66.
21. Branson, D. E., and Ozell, A. M., "Camber in Prestressed Concrete Beams," ACI Journal, Proceedings V. 57, No. 12, June 1961, pp. 1549-1574.
22. Corley, W. G.; Sozen, M. A.; and Siess, C. P., "Time-Dependent Deflections of Prestressed Concrete Beams," Bulletin No. 307, Highway Research Board, 1961, pp. 1-25.
23. Branson, D. E., "Time-Dependent Effects in Composite Concrete Beams," ACI Journal, Proceedings V. 61, No. 2, Feb. 1964, pp. 213-230.
24. Zia, P., and Stevenson, J. F., "Creep of Concrete Under Non-Uniform Stress Distribution and its Effect on Camber of Prestressed Concrete Beams," Report of Highway Research Programme No. ERD-110-R, June 1964, pp. 1-110.
25. Sinno, R., "The Time-Dependent Deflections of Prestressed Concrete Bridge Girders," Dissertation, Texas A & M University, 1968.
26. Yang, D. D., "Creep in Prestressed Lightweight Aggregate Concrete," Dissertation, Texas A & M University, 1966.
27. Subcommittee 5, ACI Committee 435, "Deflections of Prestressed Concrete Members," ACI Journal, Proceedings V. 60, No. 12, Dec. 1963, pp. 1697-1728.
28. Branson, D. E., "Design Procedures for Computing Deflections," ACI Journal, Proceedings V. 65, No. 9, Sept. 1968, pp. 730-742.

29. Young, J. A., "Evaluation of Experimental Data Obtained from Lightweight Aggregate Bridge Girders," Report No. 1, Iowa Highway Research Board Project No. HR-104, Sept. 1968.

30. Pauw, Adrian, "Static Modulus of Elasticity of Concrete as Affected by Density," ACI Journal, Proceedings V. 57, No. 6, Dec. 1960, pp. 679-687.

31. Klieger, Paul, "Long-Time Study of Cement Performance in Concrete, Chapter 10--Progress Report on Strength and Elastic Properties of Concrete," ACI Journal, Proceedings, V. 54, No. 6, Dec. 1957, pp. 481-504.

32. Hanson, J. A., "Prestress Loss as Affected by Type of Curing," Journal, Prestressed Concrete Institute, V. 9, No. 2, Apr. 1964, pp. 69-93. Also Development Department Bulletin D75, Portland Cement Association, Skokie, Ill.

33. Meyers, B. L., Branson, D. E., and Anderson, G. H., "Creep and Shrinkage Properties of Lightweight Concrete Used in the State of Iowa," Phase I--Progress Report, Oct. 1968.

34. Magura, D. D., Sozen, M. A., and Siess, C. P., "A Study of Relaxation in Prestressing Reinforcement," Journal, Prestressed Concrete Institute, V. 9, No. 2, Apr. 1964, pp. 13-58.

35. Antill, J. M., "Relaxation Characteristics of Prestressing Tendons," Civil Engineering Transactions, The Institution of Engineers, Australia, V. CE 7, No. 2, 1965.

APPENDIX A

Materials and test specimens

The details of the concrete mix and mixing procedure for the sand-lightweight concrete used in the laboratory beams and bridge girders are shown in Table A1. Ready-mix normal weight concrete was used for the slabs. The beams, slabs, shrinkage and creep specimens, and control cylinders were moist cured for 3 days. The laboratory beams were prestressed at age 7 days and the bridge girders at age 2-3 days.

The concrete properties, temperature, and humidity data are shown in Table A1. The details of the beam cross-sections, steel content, prestress force at release, design stresses, and other pertinent information are shown in Table A2. The beams are shown in Fig. A1.

Two shrinkage specimens of the same cross-section as the beams and 2' long were cast for each sand-lightweight concrete. A 20" by 20" slab was cast to obtain shrinkage strains for each normal weight concrete. A stack of three 6" by 12" cylinders was placed under a sustained uniform stress of about 30% of the ultimate concrete strength to obtain creep data for each sand-lightweight concrete. The creep and shrinkage data for the sand-lightweight concrete are shown in Figs. 5 and 6.

Various stages in the preparation and testing of the specimens are shown in Figs. A2 through A9.





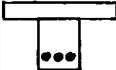
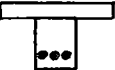

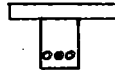
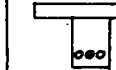
Instrumentation and test data

Steel collars with electrical strain gages (SR-4) mounted thereon were used as load cells for individual strands to measure the prestressing

TABLE A1--DETAILS OF CONCRETE MIX AND MIXING PROCEDURE FOR
SAND-LIGHTWEIGHT CONCRETE USED IN PRESTRESSED BEAMS

<u>MIX DESIGN OBJECTIVES</u>	
Concrete Quantity	1½ cu. yds.
Concrete Strength at 28 Days	5000 psi
Unit Weight in Plastic State	(120 to 123) pcf
Air Entrainment	(5 ± 1) %
<u>MIX INGREDIENTS</u>	
Cement (Type I)	1058 lbs
Sand	2093 lbs
Idealite Aggregate (Contains 60% of 3/4" to 5/16" and 40% of 5/16" to #8)	1230 lbs
Water	52.5 gals
Darex @ 7/8 oz. per sack	9.75 oz
WRDA (Used instead of 31.5 oz. of pozzolith for lab. beams)	75.0 oz
<u>MIXING PROCEDURE</u>	
1. Proportion and batch sand and Idealite	
2. Add 26 gallons of water	
3. Mix for approximately two minutes	
4. Proportion and batch the cement	
5. Add six gallons of water	
6. Add Darex AEA in 3 gallons of water	
7. Add WRDA with the remaining water while adjusting to a 2½ " slump	

TABLE A2--DETAILS OF TEST BEAMS IN GROUPS A, B, AND C

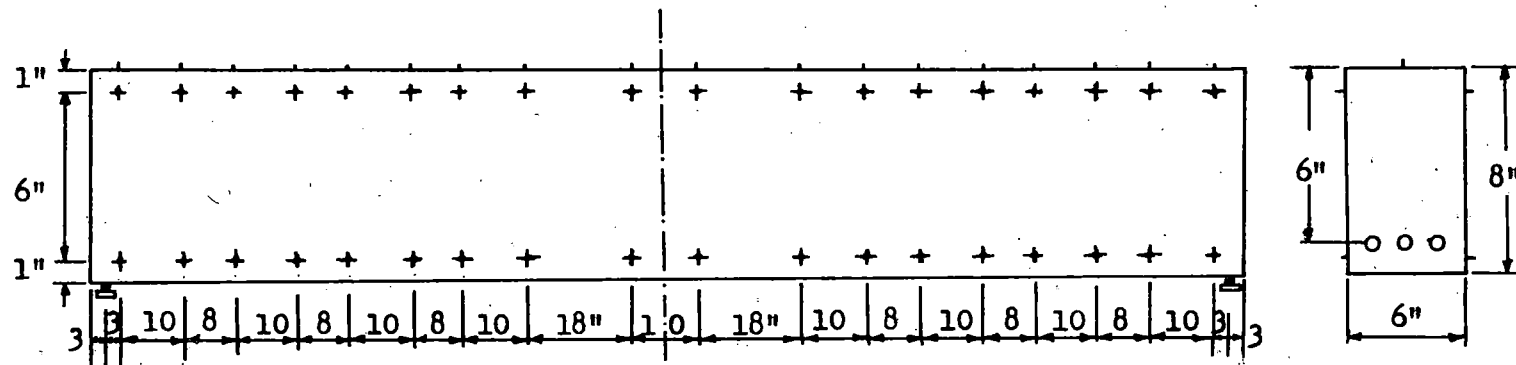
	¹ All Beams are 6" by 8", d = 6", Spans are 15.0', ² Slabs are 20" by 2"								
Beam Group	Group A			Group B			Group C		
Beam No.	A1	A2	A3	B1	B2	B3	C1	C2	C3
Beam			³ 						
Prestressing Strand Dia. in	Two 3/8 One 5/16	Three 5/16	One 3/8 One 5/16	Three 5/16	Three 5/16	Three 5/16	Two 3/8 One 5/16	Two 3/8 One 5/16	Two 3/8 One 5/16
A _s in ²	0.2176	0.1734	0.1377	0.1734	0.1734	0.1734	0.2176	0.2176	0.2176
p = A _s /bd	0.0060	0.0048	0.0038	0.0048	0.0048	0.0048	0.0060	0.0060	0.0060
Design Prestress Force, F _i kips	38.0	30.0	24.0	30.0	30.0	30.0	38.0	38.0	38.0
Measured F _i kips	37.0	29.6	23.4	30.0	29.9	29.9	38.0	37.9	37.9
⁴ Concrete stresses at release at end of beam psi	t= +388 b=-1932	t= +311 b=-1541	t= +244 b=-1224	t= +313 b=-1563	t= +312 b=-1555	t= +312 b=-1555	t= +395 b=-1975	t= +394 b=-1970	t= +394 b=-1970

¹ • 3/8" Strand, • 5/16" Strand, Measured stress in all strands = (172 ± 4) ksi.

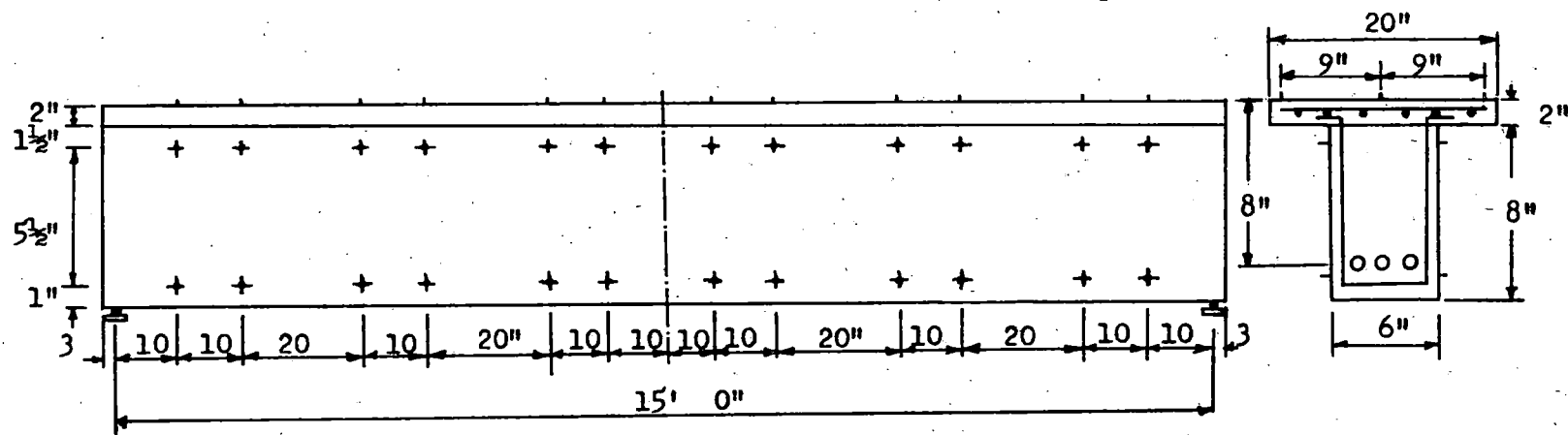
²Six gage WWF, 6" by 6" (A_s = 0.058 in² per ft width), slab steel placed in center of slab section. No. 3 U-Stirrups in form of ties for composite slab are spaced at 6" cc. in end quarter-span and at 22½" cc. in middle half of beam.

³Strands placed so that lateral eccentricity is eliminated.

⁴These stresses are computed using the Measured F_o: t = top fiber stress, b = bottom fiber stress. These initial stresses refer to the rectangular section in all cases. The rectangular (6" by 8") beam dead load, extreme fiber stress at midspan = 218 psi.



Non-composite beam and gage point locations for beams of Group A



Composite beam and gage point locations for beams of Groups B and C. The location of the strain gage points on the side of the beam also refer to non-composite beams B1 and C1

Fig.A1--Non-composite and composite test beams and location of strain gage points

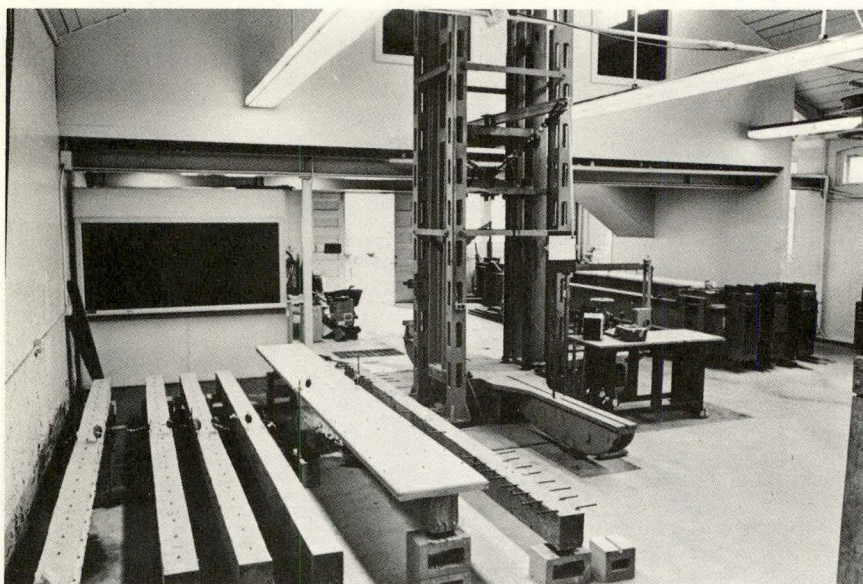


Fig. A2--View of laboratory showing beams in foreground and prestressing bed containing additional beams at right. Two additional composite slabs (for a total of 4 composite beams) have since been cast

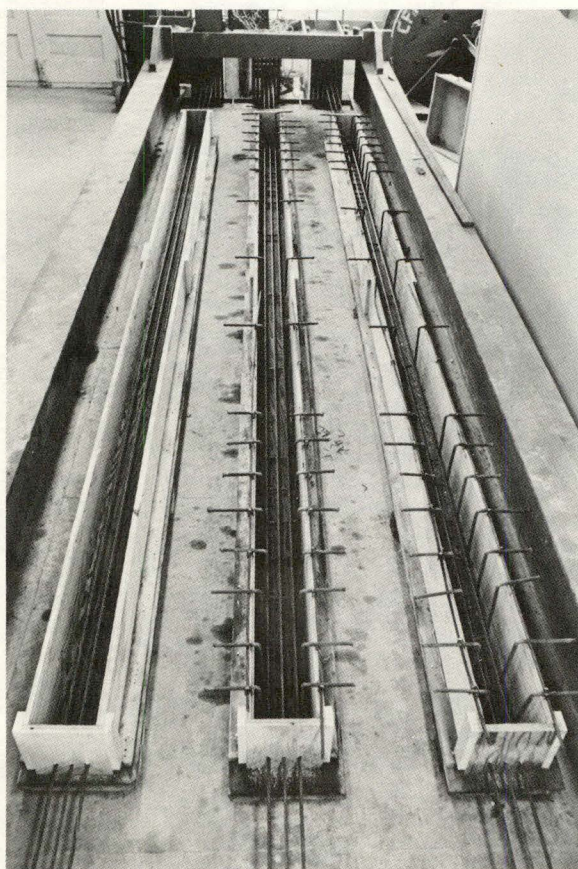


Fig. A3--Forms for beams in prestressing bed

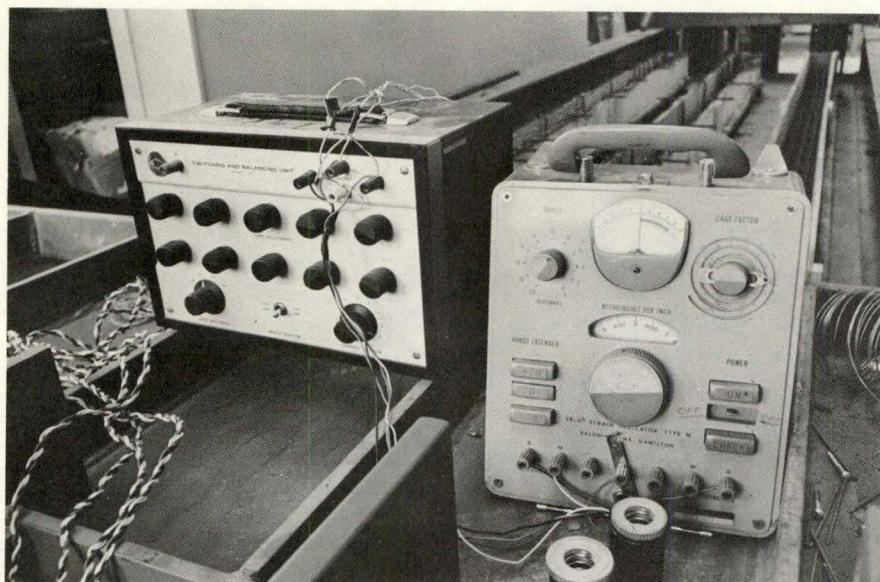


Fig. A4--Strain gage indicator and switching and balancing unit used with load cells to measure prestress force

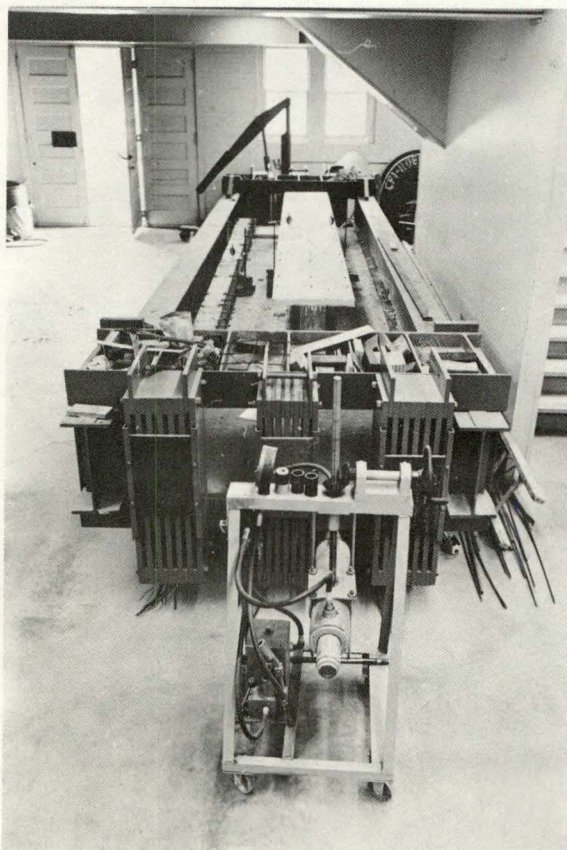


Fig. A5--Prestressing bed, jacking equipment and beams stored in bed

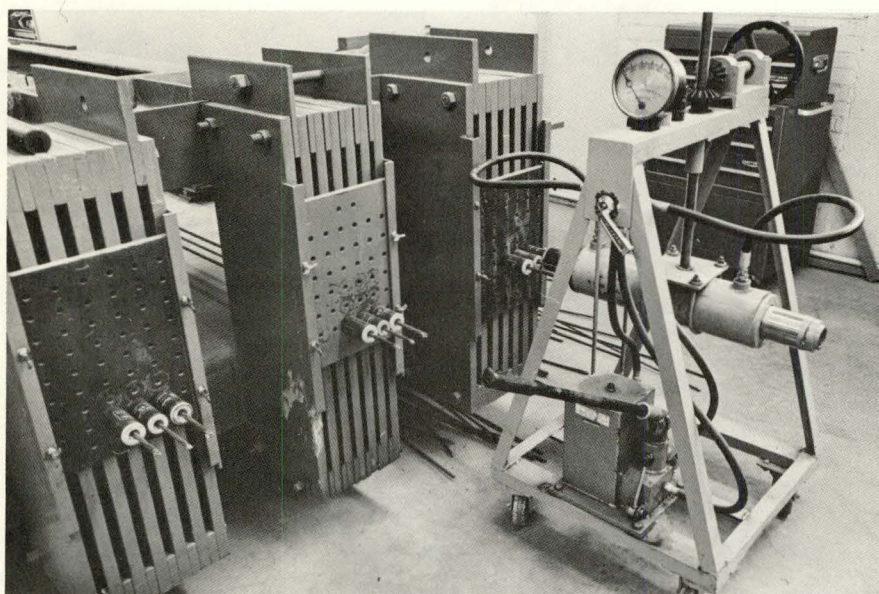


Fig. A6--Close-up of jacking equipment, bulkheads, and grips

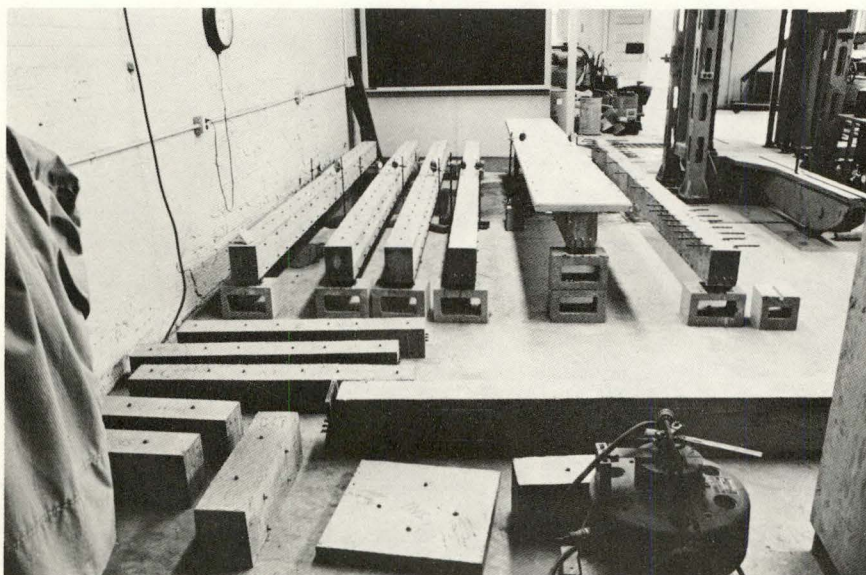


Fig. A7--Shrinkage specimens in foreground and 7 beams (1 beam crosswise in foreground). Two additional beams in prestressing bed

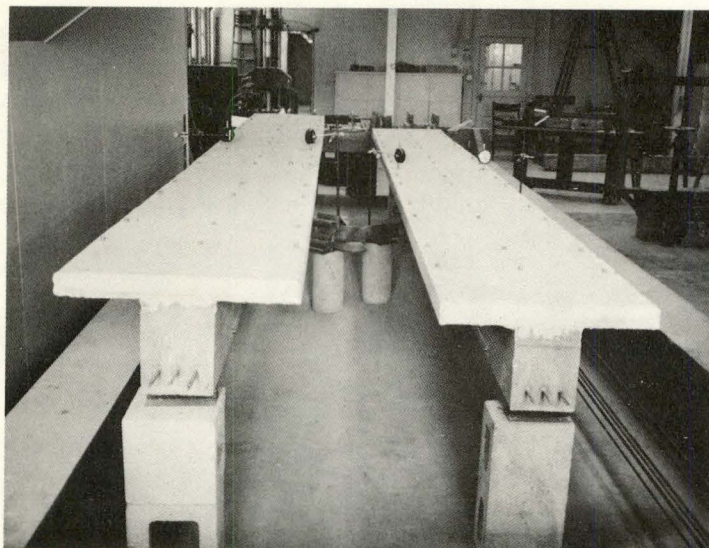


Fig. A8--Two of 4 composite beams. Strain gage points and dial gages can be seen. Strands used in relaxation tests are seen at right.

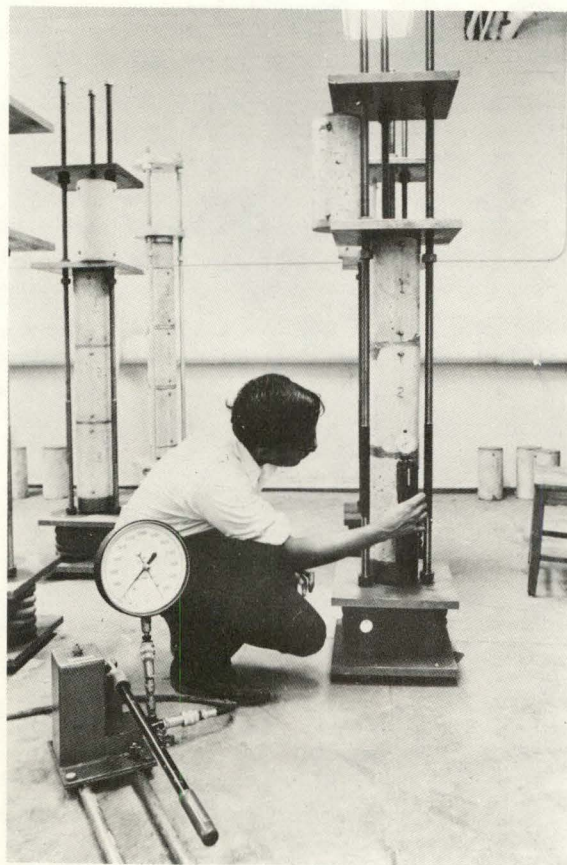


Fig. A9--Cylinders loaded in creep racks and Whittemore gage used to measure strains of beams and shrinkage and creep specimens

force applied to each beam. Dial gages were used on both sides of each beam at midspan to measure both initial and time-dependent camber. The dial gage tips were placed on the top of the beams in order to obtain "positive" camber readings. The use of two dial gages provided an indication of warping of the beams, and this was found to be negligible.

A Whittemore mechanical strain gage (10" gage length) was used to measure concrete strains. The gage points were stainless steel plugs glued to the concrete. The gages are distributed at regular intervals along both sides of the prestressed beams (near the top and bottom), along the top of the non-composite beams of Group A, and along the edges and centerline on the top of the composite slabs. The location of the gage points is shown in Fig. A1.

At the end of the time-dependent study period for the beams of Groups B and C (4 of 6 were composite beams), the load-deflection behavior under cyclic loading and up to failure was obtained. Two dial gages were used to measure the midspan deflections, and an average of the two used in each case. As in the case of the camber readings, little warping was observed. The number and relative length of cracks were photographed and studied under various stages of loading. This data is not included in this report as it is to be incorporated in the Phase 2 study of the project.

APPENDIX B

Discussion of variables affecting creep and shrinkage^{10,12,13,15,33}

Concrete undergoes time-dependent deformations under the action of sustained loads that are substantially greater than those of a corresponding unstressed specimen. These additional strains due to the effect of sustained stress are attributed to creep of the concrete. Current nomenclature regarding creep of concrete is summarized in Fig. B1.

When specimens are subjected to uniform axial stress, only normal strains (both elastic and inelastic) are usually considered. The elastic strains are stress dependent and recoverable. These strains include both time-independent and time-dependent strains. The time-independent elastic strain is also referred to as initial or instantaneous strain.

The stress independent component of the inelastic strain is normally called shrinkage. This strain is partially reversible. The stress dependent irrecoverable strains include microcracking effects as well as shrinkage or drying creep resulting from moisture migration due to applied stress. The drying creep cannot be separated from the irreversible shrinkage.

The total creep strain consists of (a) Basic creep--delayed strain due to the interaction between solid and fluid phase, (b) Drying creep--consolidation due to seepage of internal moisture, and (c) Microcracking creep--creep due to irrecoverable creep strains accompanying microcracking.

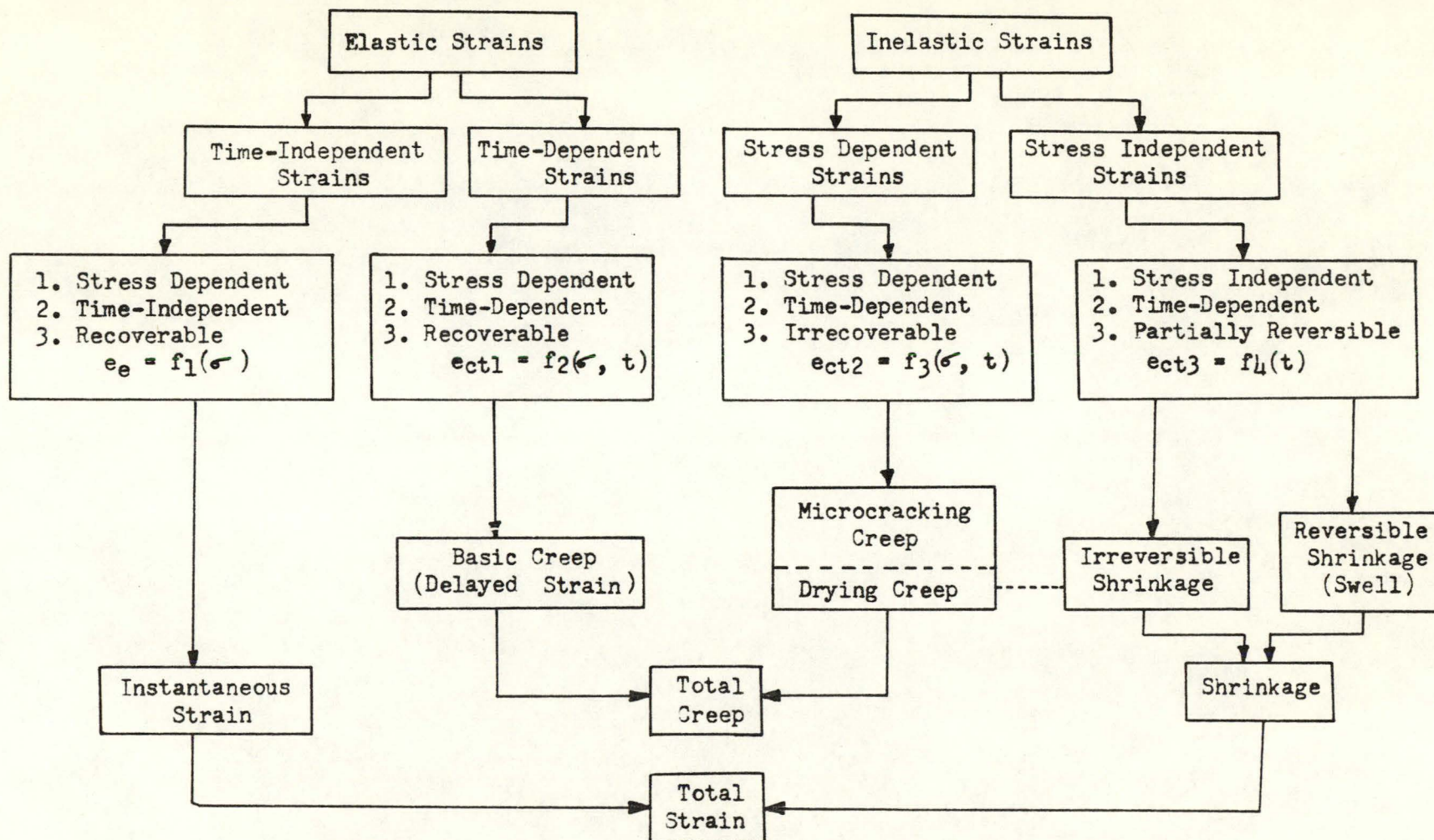


Fig.B1 --Strain Components

The recoverable strains may be time-independent (instantaneous recovery), time-dependent (delayed strain), or stress independent strain recovery (swelling). The independence of creep and shrinkage of concrete has yet to be established. However, creep and shrinkage occur simultaneously in concrete structures and, from a practical standpoint, these may be considered additive in nature. This independence is assumed through the use of companion stressed and unstressed specimens, so that the total time-dependent strain minus the free shrinkage strain is attributed to creep.

The prediction of time-dependent concrete strains is further complicated by the fact that strains and internal stresses are affected by the properties of the material as well as by curing and environmental conditions. A comprehensive study of time-dependent concrete concrete strains includes a large number of variables. These variables are summarized in Fig. B2. A detailed study of all these variables is beyond the scope of this report. However, with reference to the principal factors that effect time-dependent concrete strains, the following are considered in this report in the development of procedures for predicting creep and shrinkage:

- | | |
|--|---|
| 1.1 Minimum thickness of member | 1.4 Environmental humidity |
| 1.2 Water-cement ratio in the form of slump and cement content | 1.5 Time of initial loading and time initial shrinkage considered |
| 1.3 Mix proportions in the form of percent fines and air content | |

Parameters affecting Creep and Shrinkage Concrete Strains

- | | | | |
|-----------------------------|-------------------------|---------------------------------------|----------------------------------|
| 1. Minimum member thickness | 5. Length of curing | 9. Environment temperature | 12. Number of load cycles |
| 2. Water-Cement ratio | 6. Curing temperature | 10. Time of initial load | 13. Duration of unloading period |
| 3. Mix proportions | 7. Curing humidity | and time initial shrinkage considered | 14. Stress distribution |
| 4. Type of aggregate | 8. Environment humidity | 11. Duration of load period | 15. Stress magnitude |
| | | | 16. Stress rate |

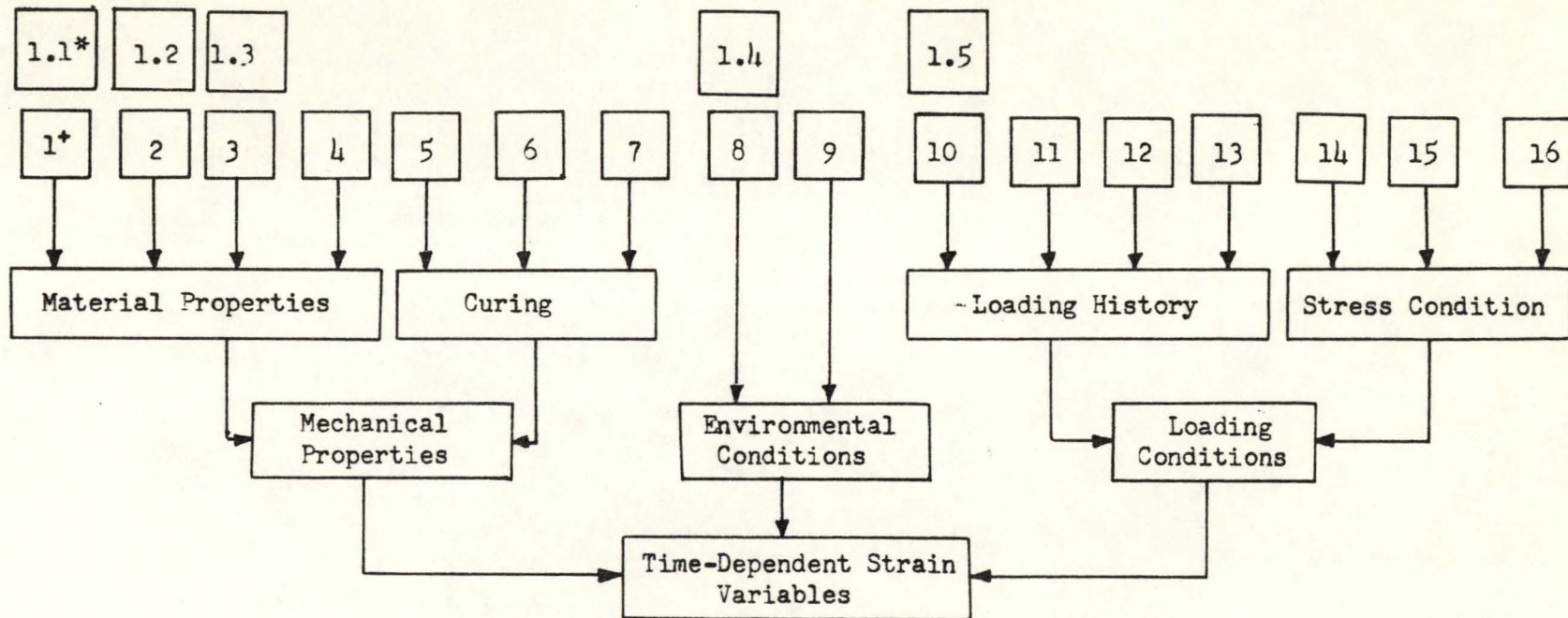


Fig. B2--Time-Dependent Strain Variables

* Parameters studied by Jones¹⁵, and used in this report
 + These numbers refer to the parameters listed above

1.1 Minimum thickness of member

Creep--Several investigators^{14,15} have indicated an influence of size of specimen on creep and shrinkage. Measured creep decreases with an increase in the size of the member, but when the specimen thickness exceeds about three feet, the size effect is no longer visible. The influence of size on creep is greatest during the initial period after the application of load. Beyond several weeks, the rate of creep is essentially the same in specimens of all sizes. The effect of member size on creep is indicated in Fig. B3.

Shrinkage--The effect of member size on shrinkage is indicated in Fig. 3. It is difficult to estimate the effect of size on the amount of shrinkage that will occur in a concrete member, since the rate and total amount of shrinkage is a function of the exposure conditions. If a member is relatively small with a large ratio of surface area to volume, it will dry out rather rapidly. However, if the member is extremely large and massive, its interior may never dry out and shrinkage may be much less.

1.2 a. Slump

Creep--The effect of increasing the slump (with water content as the only variable) on creep is indicated in Fig. B3. As the water content increases, the quality of the cement paste decreases and its relative volume increases. Since creep in concrete takes place almost entirely in the paste, the relative volume increase effects creep directly.

Shrinkage--The effect of increasing the slump (with water content as the only variable) on shrinkage is indicated in Fig. B4. The

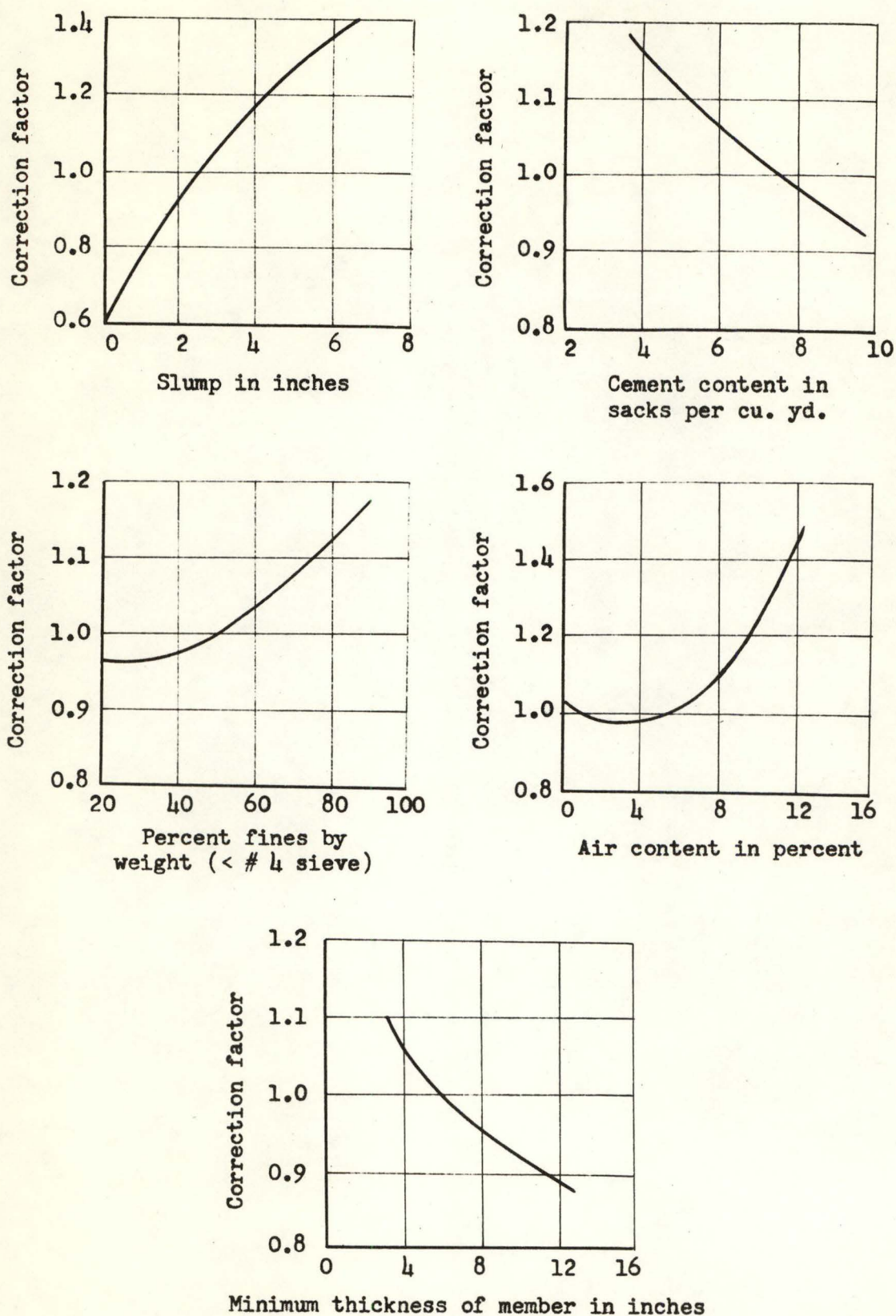


Fig. B3--Creep correction factors for slump, cement content, percent fines, air content, and minimum thickness of member, modified from Jones¹⁵

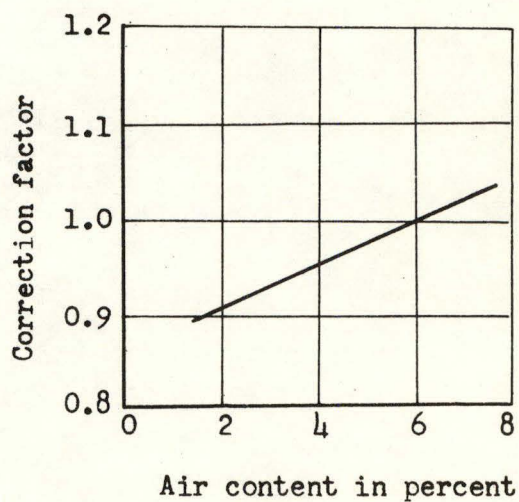
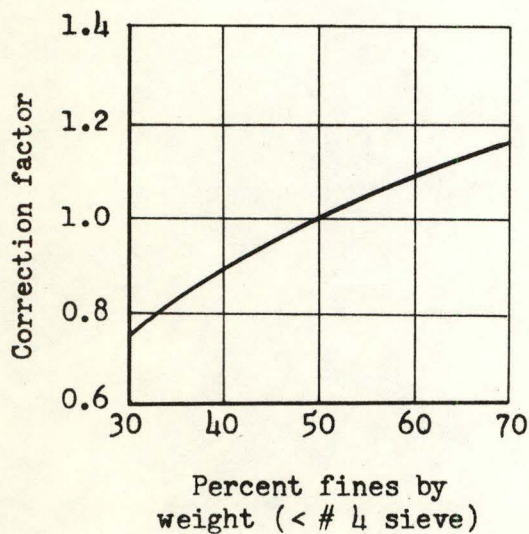
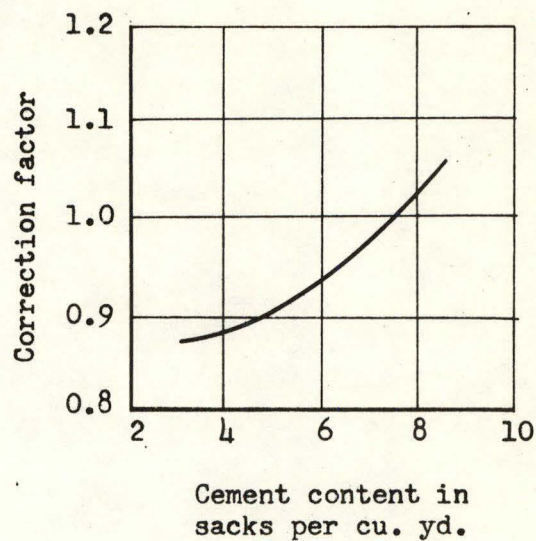
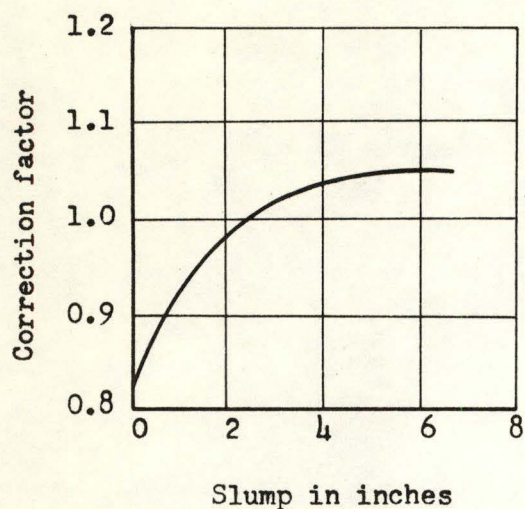


Fig. B4--Shrinkage correction factors for slump, cement content, percent fines, and air content, modified from Jones¹⁵

number of capillary voids in the cement paste increases with increasing water content and consequently, the amount of drying shrinkage is increased. Drier mixes tend to have much lower shrinkage.

1.2 b. Cement content

Creep--The effect of increasing the cement content on creep is indicated in Fig. B3. The increased quality of the paste tends to offset the increase in concrete creep that would be expected due to the larger volume of the paste, and the net result is usually a decrease in creep.

Shrinkage--The effect of increasing the cement content on shrinkage is indicated in Fig. B4. When more cement is added to a concrete batch, the relative volume of the aggregate which restrains shrinkage of the paste decreases. Hence, concrete shrinkage increases as the cement content increases.

1.3 a. Percent fines

Creep--The effect of aggregate gradation on creep is indicated in Fig. B3. An increase in the fineness of the aggregate necessitates the need for more cement paste and water (for a required slump), because of the larger volume of voids in the fines. As the fineness increases, creep increases.

Shrinkage--The effect of aggregate gradation on shrinkage is indicated in Fig. B4. As the amount of fines in a batch increases, shrinkage increases. As the fineness increases, more cement paste and water is required to produce a given slump, because of the larger surface area and total volume of the void space of the fines.

1.3 b. Air content

Creep--The effect of air content on creep is indicated in Fig. B3. Though entrained air reduces the water requirement for a given slump, it causes stress concentrations around the boundaries of the bubbles, and the result is usually an increase in the amount of creep.

Shrinkage--Fig. B4 suggests that air content does not appreciably effect shrinkage when the slump is held constant. Entrained air not only reduces the water requirement for a given slump, but also replaces some of the restraining aggregates. The net result is usually a slight increase in the amount of shrinkage.

1.4 Environmental humidity

Creep--The effect of ambient relative humidity is less pronounced on creep than on shrinkage, as indicated by the correction factors in the text of this report. Numerous tests have shown that creep increases with a decrease in the relative humidity of the surrounding medium⁹. However, the Reference¹⁰-study of mature concrete suggests that ambient relative humidity effects creep only if concrete has not reached hygral equilibrium prior to loading. The apparent influence of ambient relative humidity on creep does not act through the medium of an additional loss of water from concrete. Tests have shown that an external load does not increase water loss to the surrounding air in excess of that which takes place under similar conditions without an external load¹¹. However, from a design point of view, the factors given in this report are considered adequate to estimate the effect of ambient relative humidity on creep.

Shrinkage--Since shrinkage is essentially the expulsion of water under a vapour pressure gradient, the humidity of the surrounding air is important. The effect of ambient relative humidity is more pronounced on shrinkage than on creep, as indicated by the correction factors in the text of this report. The higher the humidity, the lower will be the shrinkage, because of the reduction in the vapour pressure gradient.

1.5 a. Time of initial loading

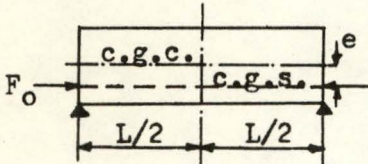
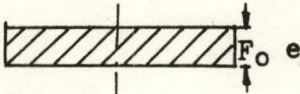
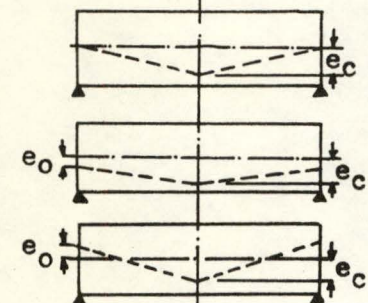
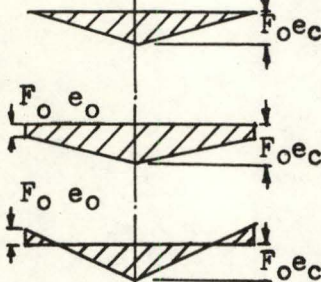
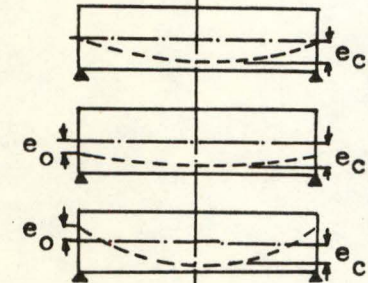
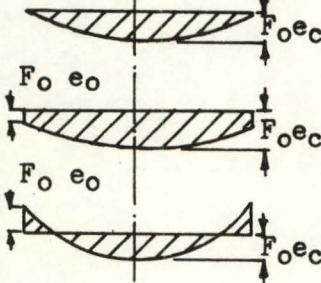
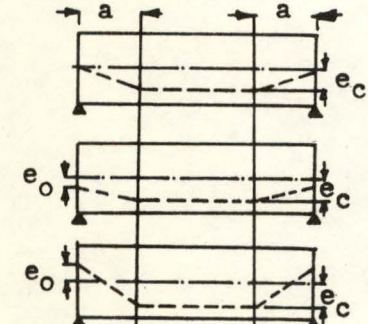
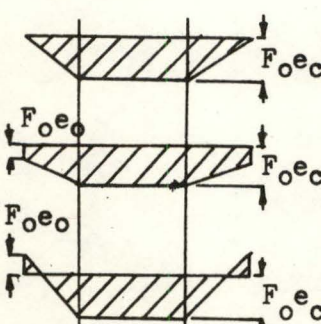
Creep--The effect of concrete age at the time of loading on creep is indicated in Fig. 2. Concrete age at the time of loading is a factor in creep behavior in so far as it influences the degree of hydration and development of strength. If concrete is loaded too early, before the cement paste has a chance to hydrate and form a cementitious material, creep may be extremely high.

1.5 b. Time initial shrinkage considered

Shrinkage--As can be seen in Figs. 4 and 7, the rate of shrinkage is quite high for early concrete ages. The total shrinkage of a structure, therefore, depends rather critically on the age of the concrete when the initial shrinkage is considered.

APPENDIX C

COMMON CASES OF PRESTRESS MOMENT DIAGRAMS WITH FORMULAS FOR COMPUTING CAMBER

Prestressed Beam	$F_o e$ Moment Diagram	Midspan Camber Due to $F_o e$ Moments
		$(\Delta_i)_{F_o} = F_o e L^2 / 8 E_{ci} I_g$
		$(\Delta_i)_{F_o} = F_o e_c L^2 / 12 E_{ci} I_g$ $(\Delta_i)_{F_o} = \frac{F_o (e_c - e_o) L^2}{12 E_{ci} I_g} + \frac{F_o e_o L^2}{8 E_{ci} I_g}$ $(\Delta_i)_{F_o} = \frac{F_o (e_c + e_o) L^2}{12 E_{ci} I_g} - \frac{F_o e_o L^2}{8 E_{ci} I_g}$
		$(\Delta_i)_{F_o} = 5 F_o e_c L^2 / 48 E_{ci} I_g$ $(\Delta_i)_{F_o} = \frac{5 F_o (e_c - e_o) L^2}{48 E_{ci} I_g} + \frac{F_o e_o L^2}{8 E_{ci} I_g}$ $(\Delta_i)_{F_o} = \frac{5 F_o (e_c + e_o) L^2}{48 E_{ci} I_g} - \frac{F_o e_o L^2}{8 E_{ci} I_g}$
		$(\Delta_i)_{F_o} = \frac{F_o e_c}{E_{ci} I_g} \left(\frac{L^2}{8} - \frac{a^2}{6} \right)$ $(\Delta_i)_{F_o} = \frac{F_o (e_c - e_o)}{E_{ci} I_g} \left(\frac{L^2}{8} - \frac{a^2}{6} \right) + \frac{F_o e_o L^2}{8 E_{ci} I_g}$ $(\Delta_i)_{F_o} = \frac{F_o (e_c + e_o)}{E_{ci} I_g} \left(\frac{L^2}{8} - \frac{a^2}{6} \right) - \frac{F_o e_o L^2}{8 E_{ci} I_g}$